공학박사 학위논문

A Study on New Approaches for Developing Process of Vibrational Characteristic Improvement by using Transmissibility:

Boundary Identification and Relative Sensitivity Analysis

진동 특성 개선을 위한 개발 과정의 새로운 접근법 연구:

결합부 특성 파악 및 상대 민감도 분석

2017년 8월

서울대학교 대학원

기계항공공학부

주 경 훈

A Study on New Approaches for Developing Process of Vibrational Characteristic Improvement by using Transmissibility:

Boundary Identification and Relative Sensitivity Analysis

by

Kyung-Hoon Joo

A Dissertation
Submitted to the Faculty of

School of Mechanical and Aerospace Engineering

at

Seoul National University

in Partial Fulfillment of
the Requirements for the Degree of

Doctor of Philosophy

August 2017

ABSTRACT

A Study on New Approaches for Developing Process of Vibrational Characteristic Improvement by using Transmissibility:

Boundary Identification and Relative Sensitivity Analysis

Kyung-Hoon Joo
School of Mechanical and Aerospace Engineering
The Graduate School
Seoul National University

When analyzing the components assembled compactly in a system for setting the shaker or measuring an impact force exerted on the component correctly, the measurement errors caused by an incorrectly measured force could be increased. Transmissibility includes only response data, unlike FRFs that include force measurements. In this thesis, new approaches for developing process of vibrational characteristic improvement that consider boundary properteis and

sensitivity of responses are presented. Transmissibility concepts is adopted to identify the boundary properties and to suggest indices for relative sensitivity analysis.

A new method for identifying boundary properties are proposed. Equation for estimating boundary properties is derived by investigating the difference in transmissibilities between a component under the coupled condition and under the free condition. Discrete multiple degrees of freedom system with single boundary and multiple boundary conditions are used to verify of the method. The method is also applied to a beam which is the simplest structural form of continuous system to investigate whether the method still usable in practical condition. Good agreement is achieved when estimated properties are compared with exact properties. Further, Error equation using measurement noise is developed to assess the robustness of the method for application under practical conditions.

In addition, indices based on the transmissibility are suggested to analyze relative sensitivity of responses. Relative senstivity of responses with respect to variables should be analyzed to make small design modifications for improving the vibrational charactertistics of a system. Two types of indices with respect to variables are developed for

indicating an appropriate position where the design variable could be modified and indicating an effect of the specific design variable on the responses. Discrete multiple degrees of freedom system and two numerical beam models are used to investigate whether the proposed indices reflect the relative changes in response to small design modifications. It has been found that the proposed indices exactly represent the sensitivity characteristics of the system by showing that the indices agreed well with the indicators for all frequency ranges.

Keywords: Transmissibility, Boundary properties, Apparent mass, Accelerance, Frequency response function, Sensitivity index, Normalized response variation

Student Number: 2011-20759

TABLE OF CONTENTS

Page

LIST OF TABLES

LIST OF FIGURES

CHAPTER 1

INTRODUCTION

Modifying the general or material properties is generally suggested to reduce or block the vibrational energy generated by a source transmitted through a structure pathway to not be incident on the target. Studies on design alternatives for resolving the vibrational problem are essential, and modified designs need to be verified in the early design phase once design alternatives are suggested, if possible. For this purpose, analyses that consider the boundary conditions and the sensitivities of responses, which play important roles in improving the vibrational characteristics of the components, are required.

System components should be analyzed under the coupled condition. The boundary model has very important properties for estimating the vibration characteristics of components coupled with the system. Note, however, that it is very difficult to define the analytical model of boundary characteristics accurately. Only a few simple conditions are possible, if at all. However, the boundary properties of real structures consist of many different types of boundary systems, and it is not possible to formulate mathematical models for all types of boundary systems. Therefore, instead of characterizing the

boundary properties directly, an experimental approach is studied as an alternative method to determine the boundary properties of a real structure by investigating the difference in vibration characteristics between a component with and without boundary properties. Thus far, studies aimed at determining the boundary properties or coupling components with the boundary have attracted much attention. To identify the boundary properties, all studies use the frequency response functions (FRFs), the most important property showing the component vibration characteristics. Tsai and Chou [1] determined the single bolt joint properties through the substructure synthesis method using equilibrium and compatibility equations on the joint coordinate. The FRFs between substructures are used to develop the idea of the proposed method. Wang and Liou [2] introduced Tsai and Chou's research to determine the joint properties more accurately by reducing the measurement noise in FRFs. Yang et al. [3] improved previous studies by considering the joint as a coupled stiffness matrix and not just as a translational spring and a rotational spring. Ren and Beards [4] had the same basic idea as other methods. However, this method was expanded to be applicable to structures connected to multiple joints, and the joint properties are considered to be composed of the mass, stiffness, and damping matrices unlike previous methods using massless spring-damper models as a joint model. The final objective of this study is to reduce the

measurement error effect. Čelič and Boltežar [5] improved Ren and Beards's theory by containing the rotational effects. They also derived a new equation for identifying the joint properties for experimental use. In the following work, they studied how coordinate reduction affects joint identification by simulating the method numerically [6]. According to this literature, insufficient FRFs of internal DOFs affect the estimation accuracy because measurement noise plays an important role in joint identification with inadequate DOFs. Thus, Wang et al. [7] developed a method of estimating unmeasured FRFs using measured FRFs. They tried to overcome the disadvantages of joint identification from insufficient information on partially measured FRFs by using additional unmeasured FRFs estimated from measured FRFs. The joint identification methods involving iteration for estimated FRFs that are to be fitted to measured FRFs have also been studied. Tol and others [8] identified the joint model using the FRF decoupling method without employing joint system FRFs and used an algorithm for updating the joint parameters by minimizing the difference between the estimated receptance and actual receptance. Cao et al. [9] proposed an FE model updating method for joint identification, which is a process of minimizing the difference between simulated FRFs and measured FRFs, in order to estimate the joint properties more accurately. Unlike approaches to identify the joint properties, as explained previously, Hwang [10] derived the

joint identification method by using the equation of motion of the structure instead of the compatibility and equilibrium conditions when a structure is attached to another connection using FRFs. This method is very simple because only the difference between the inverted FRFs of components with and without boundary properties is used for identifying the connection properties. Mehrpouya et al. [11] proposed a methodology for identifying the joint properties based on the inverse receptance coupling (IRC) method using only the translational FRFs of an assembled structure to estimate the joint FRFs and introduced the point-mass joint model to assess the error resulting from the assumption in the IRC method. In addition, many studies used modal parameters acquired from modal testing; however, as mentioned above, the difficulties in extracting modal parameters accurately are forcing researchers to use a response model for identifying the joint properties [3-11].

The component should be modified to improve the vibrational characteristics of a system with problems. A general approach involves making small design modifications to the system parameters. For this, it is necessary to analyze the relationship between the dynamic responses and the design variables. Sensitivity analysis is the study of variations of specific physical quantities with respect to the design variables, and it indicates the positions where small design modifications could be applied to improve the vibrational

characteristics. Sensitivity analysis is widely used to indicate the direction for the optimal design of a system with iterating process. The frameworks of sensitivity analysis have been studied by several researchers [12-16]. Many researches about the sensitivities of eigenvalues and eigenvectors [17-19], sensitivities of frequency responses [20-22], and sensitivities of dynamic responses [23-26] have been studied. Further, the sensitivity analysis is increasingly used in various branches of dynamic analysis such as damage detection [27, 28], model updating [29, 30], and structural-acoustic problems [31]. This article focuses on the sensitivity analysis of dynamic responses. Haug and Arora [23] developed an efficient method to calculate the derivatives of the responses of elastic structures by adopting an adjoint variable method. Zhang and Der Kiureghian [24] presented a finite element solution method for analyzing the response sensitivities of inelastic structures. Liu et al. [25] proposed a new algorithm for a more efficient calculation of the response sensitivities and Hessian matrix, with respect to earthquake excitation. Further, they [26] utilized the Gauss precise time step integration method to obtain the derivatives of the dynamic response under transient loading condition. There have been efforts to enhance the accuracy of the algorithms used for calculating the derivatives. Kirsch and Papalambros [32] adopted a combined approximation approach to develop an efficient method of approximating the

response and response derivatives. Kirsch et al. [33] developed an improved and efficient solution for calculating the displacement derivatives using global finite differences, as they can be implemented more effectively than analytical derivatives. Bogomolni et al. [34] calculated the response sensitivities using the displacement and sensitivities of eigenvectors, under dynamic loading condition. The proposed approach simplifies differential equations so that they can be solved more efficiently. Several authors have proposed the time-domain approach for the sensitivity analysis of dynamic responses. Su and Xu [35] presented an explicit time-domain formulation for dynamic responses under non-stationary random excitation. Hu et al. [36] developed a more efficient and concise expression by using the direct differentiation method.

In this thesis, transmissibility concept is applied to two subjects explained above. The transmissibility expressed by the two frequency response functions represents the ratio between two response data. Because the same force is exerted on the component, the force effect is eliminated. Therefore, it does not require the measurement of the force. Liu and Ewins [37] studied the transmissibility properties of an MDOF system that is composed of a chain-like mass-spring system. Ribeiro et al. [38] and Maia et al. [39] expanded this transmissibility concept to be more generalized for applying practical cases by introducing the input and output response matrices called as the transmissibility

matrix. These are basic studies on using the MDOF transmissibility concept in recent years. The transmissibility concept is applied to various branches of research dealing with vibration characteristics. Noumura and Yoshida [40] proposed a path contribution analysis using the transmissibility matrix instead of transfer functions showing the characteristics of paths. Because time-consuming processes of measuring FRFs and calculating the force exerted on paths do not need to be performed, this is a very attractive method. This method uses operating data. The area of operational transfer path analysis (OTPA) is still being studied by some researchers, such as Gajdatsy et al. [41, 42] Tcherniak and Schuhmacher [43], and De Klerk and Ossipov [44], for complementing the basic idea of OTPA. The transmissibility concept was also used to identify the modal parameters. Guillaume et al. [45] showed how to extract the modal parameters from only response data using the frequency-domain maximum likelihood estimator. Subsequently, unlike previous studies that used white noise as a source for identifying the modal parameters with only response data, Devriendt and Guillaume [46] suggested a new operational modal analysis (OMA) technique using transmissibility that does not need any assumption about the force so that parameters can be estimated from non-white-noise, thus reducing the possibility of wrong identification. Further studies on this topic are being reported [47-49]. In addition to the OTPA and OMA, the

concept of transmissibility is used for damage detection [50-52], force identification [53], model updating [54], predicting the transmitted force to the ground when a component is moving on flexible ground [55], estimating unmeasured FRFs [56, 57] and sensitivity analysis [58].

This thesis is organized as follows. In Chapter 2, general concept of transmissibility is introduced before applied to boundary identification and relative sensitivity analysis. The two expressions of transmissibility that can be formed by the receptance and dynamic stiffness are obtained. Further, the relation between the two definitions is also shown. In Chapter 3, the formulation of a method for identifying boundary properties as a response model is presented. The boundary properties can be estimated by comparing the characteristics of the components under three different conditions. By using the transmissibilities that are obtained from three different conditions, explicit relation between the transmissibilities and boundary characteristics is derived. The derived equation is verified using a discrete multiple degrees of freedom system with single boundary and multiple boundary conditions and by application to a beam, which is the simplest continuous structural form to validate the feasibility of the theory. The transmissibility defined by the apparent mass matrix is used for verifying the derived equation for identifying the boundary properties in the discrete system. However, when applying the

equation to practical cases, as is the purpose of this research, the transmissibility matrix should be defined using only the response data. For this purpose, the accelerance matrix is modified slightly to the response matrix using the input as a unit force. This transmissibility matrix composed of response data is used for validating the equation in a continuous system. Furthermore, the effects of measurement noise are also investigated to assess the robustness of the method for application under practical conditions. In Chapter 4, new sensitivity indices based on the transmissibility concept are presented for analyzing the relative sensitivity of responses with respect to the design variables that are used to indicate the sensitive positions where small design modifications can be applied and to analyze the effect of these modifications on the responses. 7-DOF discrete model is adopted to verify the indices. The indices are compared to indicators representing normalized response variations between the components before and after applying the small design modifications. Furthermore, two beam models are used to validate the indices with respect to mass and stiffness in more practical applications. Finally, conclusions of the thesis are presented in Chapter 5.

In summary, applying the transmissibilty concept to identify the boundary model and to suggest the sensitivity indices related to variables for relative sensitivity analysis are the main purpose of this thesis.

CHAPTER 2

CONCEPT OF TRANSMISSIBILITY

2.1 Introduction

In recent years, as the response data are used for identifying the system parameters and analyzing the path contribution, the transmissibility concept becomes more important in dynamic analysis. The transmissibility is the ratio between the frequency response functions when the input force is applied on the same position. The transmissibility is therefore expressed as the ratio of the two response data, excluding the force effect. Because of this advantage, many researchers tried to use the transmissibility for analyzing the dynamic characteristics of the system. The concept of transmissibility is described briefly as a basis for developing process of vibrational characteristic improvement. Two approaches to evaluate transmissibility from receptance and dynamic stiffness are described in this Chapter.

2.2 Formulation of transmissibility

There are two ways of obtaining transmissibility by using receptance and dynamic stiffness. In this section, the definitions of transmissibility are presented.

The MDOF system's equation of motion can be defined by using receptance $\mathbf{H}$

$$\mathbf{x} = \mathbf{HF}, \tag{2.1}$$

where $\mathbf{x}$, $\mathbf{H}$, and $\mathbf{F}$ are the displacement, receptance, and Force, respectively. Consider the schematic model composed of three different coordinates as shown in Fig. 2.1. If external forces are applied to coordinate k, displacements at coordinate a is expressed as

$$\mathbf{x}_a = \mathbf{H}_{ak}\mathbf{F}_k, \tag{2.2}$$

where $\mathbf{H}_{ak}$ is receptance matrix between coordinates k and a. In the same way, displacements at coordinate b is also expressed as

$$\mathbf{x}_b = \mathbf{H}_{bk}\mathbf{F}_k, \tag{2.3}$$

where $\mathbf{H}_{bk}$ is receptance matrix between coordinates k and b. Rearranging Eq. (2.2) by multiplying pseudo-inverse of $\mathbf{H}_{ak}$ to eliminate the applied force at coordinate k in Eq. (2.3) gives

$$(\mathbf{H}_{ak})^{+}\mathbf{x}_a = \mathbf{F}_k. \tag{2.4}$$

Substitute Eq. (2.4) for Eq. (2.3) to obtain the relation between diplacements

at coordinate a and coordinate b.

$$\mathbf{x}_b = \mathbf{H}_{bk}(\mathbf{H}_{ak})^{+}\mathbf{x}_a. \tag{2.5}$$

The transmissibility can be defined as

$$\mathbf{T}_{ba,f_k} = \mathbf{H}_{bk}(\mathbf{H}_{ak})^{+}. \tag{2.6}$$

$\mathbf{T}_{ba,f_k}$ is the transmissibility of the displacement between the coordinate a and coordinate b when the external forces are exerted on coordinate k. $\mathbf{x}_a$ and $\mathbf{x}_b$ can be related by using transmissibility

$$\mathbf{x}_b = \mathbf{T}_{ba,f_k}\mathbf{x}_a. \tag{2.7}$$

Transmissibility also could be expressed by using dynamic stiffness. The equation of motion can be described as

$$\mathbf{Z}\mathbf{x} = \mathbf{F}, \tag{2.8}$$

where $\mathbf{Z}$, $\mathbf{x}$, and $\mathbf{F}$ are dynamic stiffness, displacement, and Force, respectively. Consider the schematic model composed of four different coordinates as shown in Fig. 2.2. Coordinates a and b are subsets related to displacements while coordinates k and l are subsets where external forces can be applied. Eq. (2.8) can be expressed as

$$\begin{bmatrix}\mathbf{Z}_{ka} & \mathbf{Z}_{kb}\\ \mathbf{Z}_{la} & \mathbf{Z}_{lb}\end{bmatrix}\begin{Bmatrix}\mathbf{x}_a\\ \mathbf{x}_b\end{Bmatrix} = \begin{Bmatrix}\mathbf{F}_k\\ \mathbf{F}_l\end{Bmatrix}. \tag{2.9}$$

Assume that the external forces are only applied to cooridnate k and there are no external forces on coorinate l. It is possible to obtain following equation from Eq. (2.9) by using $\mathbf{F}_l = \mathbf{0}$.

$$\mathbf{Z}_{la}\mathbf{x}_a + \mathbf{Z}_{lb}\mathbf{x}_b = \mathbf{0}. \tag{2.10}$$

Rearranging Eq. (2.10) to obtain the transmissibility

$$\mathbf{x}_b = -(\mathbf{Z}_{lb})^{+}\mathbf{Z}_{la}\mathbf{x}_a. \tag{2.11}$$

The transmissibility can be defined as

$$\mathbf{T}_{ba,f_k} = -(\mathbf{Z}_{lb})^{+}\mathbf{Z}_{la}. \tag{2.12}$$

$\mathbf{T}_{ba,f_k}$ expressed by dynamic stiffness is obtained.

$$\mathbf{T}_{ba,f_k} = -(\mathbf{Z}_{lb})^{+}\mathbf{Z}_{la} = \mathbf{H}_{bk}(\mathbf{H}_{ak})^{+}. \tag{2.12}$$

Finally, the tranmissibility is expressed by using dynamic stiffness and receptance. Note that the receptance matrices between coordinates related to displacement and coordinate where the external forces are applied are used while the dynamic stiffness matrices between the coordinates related to displacement and the coordinate where the external forces are not applied are used.

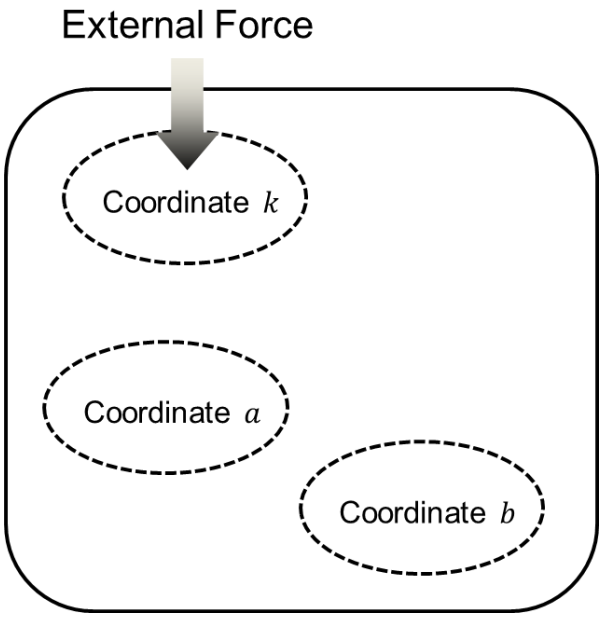

Figure 2.1 Schematic model composed of three different coordinates

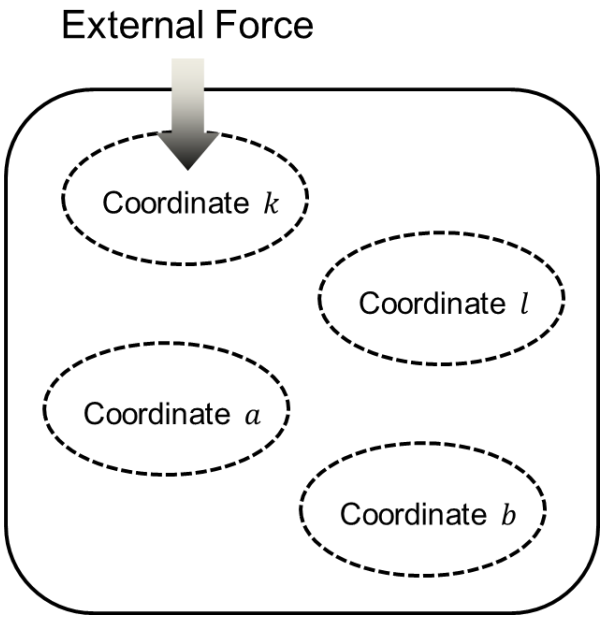

Figure 2.2 Schematic model composed of four different coordinates

CHAPTER 3

IDENTIFICATION OF BOUNDARY CHARACTERISTICS USING TRANSMISSIBILITY

3.1 Introduction

As described in Chapter 1, all methods use FRFs for developing the theory, even though the idea of the research is slightly different. In this Chapter, a new approach to determine the boundary characteristics using transmissibility composed of only the response data is suggested and validated. An explicit relation between the transmissibility concept and the boundary characteristic matrix is derived. FRFs, of course, are very important data for analyzing the vibration characteristics of a component theoretically. However, in practice, many difficult cases are encountered when measuring an input force exerted on a component connected to a full system. As a result, the input force can be measured incorrectly based on who excites a component. However, the force effects are excluded by using the transmissibility. This means that the force should be excited; however, it does not need to be measured. Even if the force is excited in the wrong direction, it does not matter if the distributed force

exciting the right direction is enough to excite the component. Consequently, less experimental errors are included in the transmissibility than in FRFs as long as the sensors for measuring the response data are installed properly.

The objective of this Chapter is to suggest a new approach for identifying the boundary characteristics using the transmissibility. Three types of transmissibilities are needed for identifying the boundary properties from the equation derived from the theory. These conditions are as follows:

(1) Free condition.

(2) Connected to boundary condition.

(3) Connected to boundary condition with mass modification.

The proposed method is applicable for almost all boundary conditions as far as sensors can be attached. The identified matrix gives the response model properties of the boundary conditions.

The method is validated using discrete models containing a single boundary condition and multiple boundary conditions. Estimating the single boundary constant is a very simple and intuitive process, unlike the multiple boundary constant estimation using the transmissibility matrix. Validations with discrete models show very obvious results. The boundary characteristic matrix can be identified exactly from the proposed method. In sequence, the continuous model of a real structure beam is used to demonstrate the numerical

validity of the method. After estimating the boundary properties, the boundary characteristic matrix (BCM) can be applied to the modified component with the free condition that could be obtained from the finite element model in the early design phase before making the real product using the equation for estimating the FRFs of modified component connected to boundary.

3.2 FRF Estimation using Boundary Properties

The FRFs of the component connected to the boundary can be estimated by the method coupling substructures A and B [59, 60]. The admittance of substructure B in the interface could be considered to substitute for the boundary conditions. Therefore, it can be explained by the following process.

The MDOF system's equation of motion is

$$\mathbf{M}\ddot{\mathbf{x}} + \mathbf{C}\dot{\mathbf{x}} + (\mathrm{j}\mathbf{D} + \mathbf{K})\mathbf{x} = \mathbf{F}, \tag{3.1}$$

where $\mathbf{M}$, $\mathbf{C}$, $\mathbf{D}$, $\mathbf{K}$, $\ddot{\mathbf{x}}$, $\dot{\mathbf{x}}$, and $\mathbf{x}$ are the mass, viscous damping, structural damping, stiffness, acceleration, velocity, and displacement, respectively.

$$\left(\mathbf{M} - \frac{\mathbf{K}_{\mathrm{eq}}}{\omega^2}\right)\mathbf{a} = \mathbf{F}, \tag{3.2}$$

where

$$\mathbf{K}_{\mathrm{eq}} = \mathrm{j}\omega\mathbf{C} + \mathrm{j}\mathbf{D} + \mathbf{K}. \tag{3.3}$$

The complex stiffness $\mathbf{K}_{\mathrm{eq}}$ containing the viscous damping, structural

damping, and stiffness is used for simplifying the equation.

The MDOF system's equation of motion can be also defined using accelerance $\mathbf{H}$,

$$\mathbf{a} = \mathbf{HF}. \tag{3.4}$$

Multiplying inversion of $\mathbf{H}$ to Eq. (3.4) yields

$$\mathbf{H}^{-1}\mathbf{a} = \mathbf{F}. \tag{3.5}$$

Then, the apparent mass $\mathbf{M}_{\text{app}}$ is expressed as

$$\left(\mathbf{M} - \frac{\mathbf{K}_{\text{eq}}}{\omega^2}\right) = \mathbf{H}^{-1}. \tag{3.6}$$

The boundary properties can be applied to the apparent mass in the free condition composed of system parameters for determining the component FRFs connected to the boundary. In this Chapter, the matrix of the boundary properties is called the BCM. Therefore, the apparent mass connected to the boundary is given by

$$\mathbf{M}_{\text{app,free}} + \mathbf{BCM} = \mathbf{M}_{\text{app,bc}}. \tag{3.7}$$

The subscript ``free'' represents the free condition and the subscript ``bc'', the connected to boundary condition. The apparent mass of the component and the inversion of the component accelerance matrix applied to the boundary condition is obtained by using the apparent mass of the free condition and BCM. By the reinversion of $\mathbf{M}_{\text{app,bc}}$, the accelerance of the component connected to the boundary can be estimated as

$$\left(\mathbf{M}_{\text{app,bc}}\right)^{-1} = \mathbf{H}_{\text{bc}}. \tag{3.8}$$

The main objective of this Chapter is to define the boundary properties using the transmissibility.

3.3 Theoretical Formulation for Estimation of Boundary characteristic matrix

Many studies have identified the joint properties using experimental data. However, all methods use the FRF data, which is thought to be easily measurable through experiments. In this section, transmissibilities obtained using only the response data are used for deriving an equation to identify the boundary properties. The newly proposed method for defining the BCM needs three types of transmissibilities obtained under different conditions: (1) free condition, (2) connected to boundary condition, and (3) connected to boundary condition with mass modification. The boundary properties can be estimated with these transmissibility data.

Consider the model schematically illustrated in Fig. 3.1, where two coordinate sets defined as non-boundary set i and boundary set j constitute the model coordinates. The governing equations for the structure having two coordinates are expressed as

$$\begin{bmatrix} \mathbf{M}_{\mathrm{app}_{ii}} & \mathbf{M}_{\mathrm{app}_{ij}} \\ \mathbf{M}_{\mathrm{app}_{ji}} & \mathbf{M}_{\mathrm{app}_{jj}} \end{bmatrix} \begin{Bmatrix} \mathbf{a}_i \\ \mathbf{a}_j \end{Bmatrix} = \begin{Bmatrix} \mathbf{F}_i \\ \mathbf{F}_j \end{Bmatrix}. \tag{3.9}$$

$\mathbf{M}_{\mathrm{app}_{ij}}$ is the apparent mass matrix between coordinates i and j. Assume that the force is exerted on non-boundary sets and there is no external force on the boundary sets. Only the internal force $\mathbf{F}_j$ arise because of the boundary condition. When the component is in the free condition, where $\mathbf{F}_j = \mathbf{0}$,

$$\mathbf{M}_{\mathrm{app}_{ji}}\mathbf{a}_i + \mathbf{M}_{\mathrm{app}_{jj}}\mathbf{a}_j = \mathbf{0}. \tag{3.10}$$

Eq. (3.10) can be rearranged to obtain the transmissibility

$$\mathbf{a}_i = -\left(\mathbf{M}_{\mathrm{app}_{ji}}\right)^{+} \mathbf{M}_{\mathrm{app}_{jj}}\mathbf{a}_j. \tag{3.11}$$

Then, $\mathbf{T}_{ij,\mathrm{free}}$ can be defined as

$$\mathbf{T}_{ij,\mathrm{free}} = -\left(\mathbf{M}_{\mathrm{app}_{ji}}\right)^{+} \mathbf{M}_{\mathrm{app}_{jj}}. \tag{3.12}$$

$\mathbf{T}_{ij,\mathrm{free}}$ is the transmissibility of the acceleration between the boundary sets of free condition and non-boundary sets when the force is exerted on non-boundary sets.

When the component is connected to the boundary, the reaction force $\mathbf{F}_j$ arises because of the existence of the boundary model composed of system parameters. Eq. (3.10) is changed as

$$\mathbf{M}_{\mathrm{app}_{ji}}\mathbf{a}_i + \mathbf{M}_{\mathrm{app}_{jj}}\mathbf{a}_j = -\mathbf{F}_j. \tag{3.13}$$

Rearranging Eq. (3.13) in terms of transmissibility gives

$$\mathbf{a}_i = -\left(\mathbf{M}_{\mathrm{app}_{ji}}\right)^{+}\left(\mathbf{F}_j + \mathbf{M}_{\mathrm{app}_{jj}}\mathbf{a}_j\right). \tag{3.14}$$

The transmissibility of the component connected to the boundary has another term composed of the reaction force, unlike the free condition component transmissibility. The term composed of the reaction force can be considered as the modified component properties of boundary sets by rearranging Eq. (3.14) as

$$\mathbf{a}_i = -\left(\mathbf{M}_{\mathrm{app}_{ji}}\right)^{+}\left(\mathbf{F}_j \frac{\mathbf{1}}{|\mathbf{a}_j|^{\mathbf{2}}}\mathbf{a}_j{}^{\mathrm{T}} + \mathbf{M}_{\mathrm{app}_{jj}}\right)\mathbf{a}_j. \tag{3.15}$$

Then, $\mathbf{T}_{ij,\mathrm{bc}}$ can be defined as

$$\mathbf{T}_{ij,\mathrm{bc}} = -\left(\mathbf{M}_{\mathrm{app}_{ji}}\right)^{+}\left(\mathbf{F}_j \frac{\mathbf{1}}{|\mathbf{a}_j|^{\mathbf{2}}}\mathbf{a}_j{}^{\mathrm{T}} + \mathbf{M}_{\mathrm{app}_{jj}}\right). \tag{3.16}$$

By considering $\mathbf{F}_j \frac{\mathbf{1}}{|\mathbf{a}_j|^{\mathbf{2}}}\mathbf{a}_j{}^{\mathrm{T}}$ as $\Delta\mathbf{M}_{\mathrm{app}_{jj}}$, $\mathbf{T}_{ij,\mathrm{bc}}$ is changed to

$$\mathbf{T}_{ij,\mathrm{bc}} = -\left(\mathbf{M}_{\mathrm{app}_{ji}}\right)^{+}\left(\Delta\mathbf{M}_{\mathrm{app}_{jj}} + \mathbf{M}_{\mathrm{app}_{jj}}\right). \tag{3.17}$$

$\mathbf{T}_{ij,\mathrm{bc}}$ can be expressed using the variation of $\mathbf{M}_{\mathrm{app}_{jj}}$. In other words, the boundary sets of the component connected to the boundary are changed to the boundary sets of the modified component in the free condition. This means that the apparent mass of the component connected to the boundary can be easily modified from the apparent mass of the free condition by adding variation to the boundary coordinate sets.

To eliminate terms other than $\Delta\mathbf{M}_{\mathrm{app}_{jj}}$, subtract Eq. (3.17) from Eq. (3.12),

$$\mathbf{T}_{ij,\mathrm{free}} - \mathbf{T}_{ij,\mathrm{bc}} = \left(\mathbf{M}_{\mathrm{app}_{ji}}\right)^{+} \Delta\mathbf{M}_{\mathrm{app}_{jj}}. \tag{3.18}$$

However, $\mathbf{M}_{\mathrm{app}_{ji}}$ still exists. It should be eliminated so that $\Delta\mathbf{M}_{\mathrm{app}_{jj}}$ can be estimated using only the response data. The mass modification technique is introduced for eliminating $\mathbf{M}_{\mathrm{app}_{ji}}$ by giving more information about the dynamic characteristics of the component. Only adding some mass on the boundary sets is required. By the same method as that for obtaining $\mathbf{T}_{ij,\mathrm{bc}}$, the transmissibility of the component connected to the boundary with mass modification on boundary sets can be derived by adding mass, $\Delta\mathbf{m}_{jj}$, to boundary sets of apparent mass

$$\mathbf{M}_{\mathrm{app}_{ji}}\mathbf{a}_i + \left(\mathbf{M}_{\mathrm{app}_{jj}} + \Delta\mathbf{m}_{jj}\right)\mathbf{a}_j = -\mathbf{F}_j. \tag{3.19}$$

Eq. (3.19) can be rearranged to obtain the transmissibility

$$\mathbf{a}_i = -\left(\mathbf{M}_{\mathrm{app}_{ji}}\right)^{+}\left(\mathbf{F}_j \frac{\mathbf{1}}{|\mathbf{a}_j|^2}\mathbf{a}_j{}^{\mathrm{T}} + \mathbf{M}_{\mathrm{app}_{jj}} + \Delta\mathbf{m}_{jj}\right)\mathbf{a}_j. \tag{3.20}$$

By using $\mathbf{F}_j \frac{\mathbf{1}}{|\mathbf{a}_j|^2}\mathbf{a}_j{}^{\mathrm{T}} = \Delta\mathbf{M}_{\mathrm{app}_{jj}}$,

$$\mathbf{T}_{ij,\mathrm{bcmm}} = -\left(\mathbf{M}_{\mathrm{app}_{ji}}\right)^{+}\left(\Delta\mathbf{M}_{\mathrm{app}_{jj}} + \mathbf{M}_{\mathrm{app}_{jj}} + \Delta\mathbf{m}_{jj}\right). \tag{3.21}$$

$\mathbf{T}_{ij,\mathrm{bcmm}}$ is the transmissibility of the acceleration between the boundary sets with mass modification and non-boundary sets.

Subtract Eq. (3.21) from Eq. (3.12)

$$\mathbf{T}_{ij,\text{free}} - \mathbf{T}_{ij,\text{bcmm}} = \left(\mathbf{M}_{\text{app}\,ji}\right)^{+}\left(\Delta\mathbf{M}_{\text{app}\,jj} + \Delta\mathbf{m}_{jj}\right). \tag{3.22}$$

Eq. (3.18) is modified to substitute $\left(\mathbf{M}_{\text{app}\,ji}\right)^{+}$ in Eq. (3.22),

$$\left(\mathbf{T}_{ij,\text{free}} - \mathbf{T}_{ij,\text{bc}}\right)\left(\Delta\mathbf{M}_{\text{app}\,jj}\right)^{-1} = \left(\mathbf{M}_{\text{app}\,ji}\right)^{+}. \tag{3.23}$$

Substitute Eq. (3.23) for Eq. (3.22)

$$\mathbf{T}_{ij,\text{free}} - \mathbf{T}_{ij,\text{bcmm}} = \left(\mathbf{T}_{ij,\text{free}} - \mathbf{T}_{ij,\text{bc}}\right)\left(\Delta\mathbf{M}_{\text{app}\,jj}\right)^{-1}\left(\Delta\mathbf{M}_{\text{app}\,jj} + \Delta\mathbf{m}_{jj}\right). \tag{3.24}$$

$$\left(\mathbf{T}_{ij,\text{free}} - \mathbf{T}_{ij,\text{bc}}\right)^{+}\left(\mathbf{T}_{ij,\text{free}} - \mathbf{T}_{ij,\text{bcmm}}\right) = \mathbf{I} + \left(\Delta\mathbf{M}_{\text{app}\,jj}\right)\Delta\mathbf{m}_{jj}, \tag{3.25}$$

where $\mathbf{I}$ is the identity matrix. Then, $\Delta\mathbf{M}_{\text{app}\,jj}$ can be derived as

$$\Delta\mathbf{M}_{\text{app}\,jj} = \Delta\mathbf{m}_{jj}\left\{\left(\mathbf{T}_{ij,\text{free}} - \mathbf{T}_{ij,\text{bc}}\right)^{+}\left(\mathbf{T}_{ij,\text{free}} - \mathbf{T}_{ij,\text{bcmm}}\right) - \mathbf{I}\right\}^{-1}. \tag{3.26}$$

Finally, one can obtain

$$\Delta\mathbf{M}_{\text{app}\,jj} = \Delta\mathbf{m}_{jj}\left(\mathbf{T}_{ij,\text{bc}} - \mathbf{T}_{ij,\text{bcmm}}\right)^{+}\left(\mathbf{T}_{ij,\text{free}} - \mathbf{T}_{ij,\text{bc}}\right). \tag{3.27}$$

By multiplying $-\omega^2$ with the BCM $\Delta\mathbf{M}_{\text{app}\,jj}$, the boundary properties can be identified as $-\omega^2\Delta\mathbf{M}_{\text{app}\,jj}$.

In short, the BCM is estimated by the proposed method using three types of transmissibilities of the component. Before applying the proposed method to practical cases, the dimensions of the coordinate sets are considered [61]. The non-boundary coordinate sets $\#i$ should outnumber the boundary coordinated sets $\#j$ at least for calculating the matrix operation.

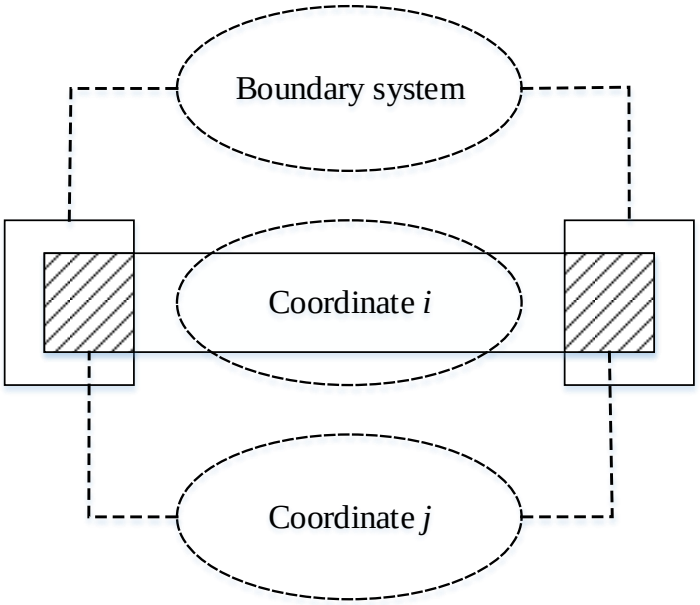

Figure 3.1 Schematic model of component connected to boundary

3.4 Verification and Application Examples

To verify the proposed method, numerical studies are performed. The method is verified on an MDOF system with a single boundary condition for better understanding the procedure intuitively. Then, it is expanded to a system with multiple boundary conditions using the transmissibility matrix. Two types of discrete systems are adopted.

(1) 2-DOF discrete system with single boundary condition

(2) 4-DOF discrete system with multiple boundary conditions

Subsequently, a finite beam model is adopted for identifying whether the method is still usable in a continuous system through a simulation.

3.4.1 Verification: 2-DOF Discrete System with Single Boundary Condition

A 2-DOF discrete system assembled by a spring and damper is illustrated in Fig. 3.2. A single boundary property characterized by k_R is connected to mass m_2. $k_{\mathrm{eq.1}}$, the sum of k_1 and $\mathrm{j}\omega c_1$, is used for simplifying calculations in this validation. The equation of motion is

$$\begin{bmatrix} m_1 - \frac{k_{\text{eq.1}}}{\omega^2} & \frac{k_{\text{eq.1}}}{\omega^2} \\ \frac{k_{\text{eq.1}}}{\omega^2} & m_2 - \frac{k_{\text{eq.1}}}{\omega^2} \end{bmatrix} \begin{Bmatrix} a_1 \\ a_2 \end{Bmatrix} = \begin{Bmatrix} F_1 \\ F_2 \end{Bmatrix}. \tag{3.28}$$

In the free condition, where the reaction force is $F_2 = 0$,

$$\frac{k_{\text{eq.1}}}{\omega^2} a_1 + \left(m_2 - \frac{k_{\text{eq.1}}}{\omega^2} \right) a_2 = 0. \tag{3.29}$$

Thus,

$$T_{12.\text{free}} = \frac{a_1}{a_2} = \frac{\omega^2 m_2 - k_{\text{eq.1}}}{k_{\text{eq.1}}}. \tag{3.30}$$

When a 2-DOF discrete system is connected to the single boundary condition characterized by $k_{\text{eq.}R}$,

$$\frac{k_{\text{eq.1}}}{\omega^2} a_1 + \left(m_2 - \frac{k_{\text{eq.1}}}{\omega^2} - \frac{k_{\text{eq.}R}}{\omega^2} \right) a_2 = 0. \tag{3.31}$$

Note that $\frac{k_{\text{eq.}R}}{\omega^2} a_2$ represents the reaction force F_2 resulting from boundary properties. Thus, the transmissibility of the component connected to the boundary is

$$T_{12.\text{bc}} = \frac{a_1}{a_2} = \frac{\omega^2 m_2 - \left(k_{\text{eq.1}} + k_{\text{eq.}R} \right)}{k_{\text{eq.1}}}. \tag{3.32}$$

In the same way, when the component is connected to the boundary with mass modification,

$$T_{12.\text{bcmm}} = \frac{a_1}{a_2} = \frac{\omega^2 m_2 - \left(k_{\text{eq.1}} + k_{\text{eq.}R} \right) + \omega^2 m_R}{k_{\text{eq.1}}}. \tag{3.33}$$

Substituting Eqs. (3.30), (3.32), and (3.33) into Eq. (3.27) gives

$$\Delta M_{\text{app}_{22}} = m_R \left(\frac{-\omega^2 m_R}{k_{\text{eq.1}}} \right)^{-1} \left(\frac{k_{\text{eq.}R}}{k_{\text{eq.1}}} \right) = -\frac{k_{\text{eq.}R}}{\omega^2}. \tag{3.34}$$

The boundary property $k_{\text{eq.}R}$ is extracted exactly by multiplying $-\omega^2$ with $\Delta M_{\text{app}_{22}}$.

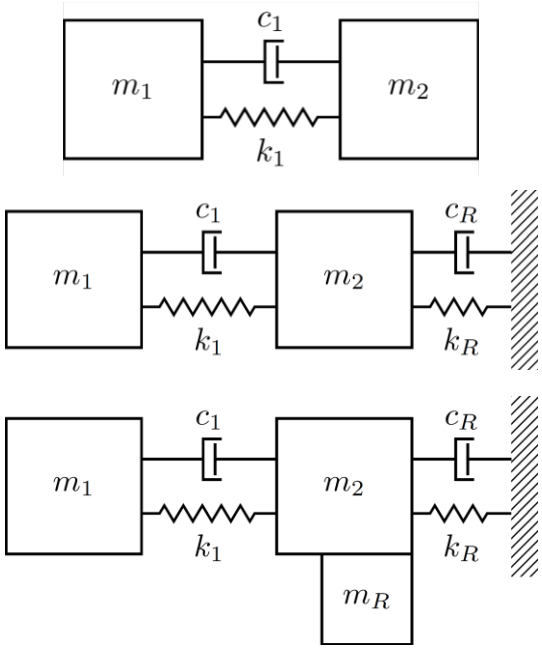

Figure 3.2 2-DOF discrete system: (a) free condition, (b) connected to boundary condition, and (c) connected to boundary condition with mass modification

3.4.2 Verification: 4-DOF Discrete System with Multiple Boundary Conditions

The 4-DOF system is illustrated in Fig. 3.3. All masses are connected to each other, and double boundary properties characterized by $k_{\mathrm{eq}.L}$ and $k_{\mathrm{eq}.R}$ are connected to mass 1 (m_1) and mass 4 (m_4), respectively. $k_{\mathrm{eq}.ij}$, the sum of k_{ij} and $\mathrm{j}\omega c_{ij}$, is used for simplifying the calculations in this validation. The apparent mass between the coordinates i and j, $\mathbf{M}_{\mathrm{app}_{ji}}$, is

$$\mathbf{M}_{\mathrm{app}_{ji}} = \begin{bmatrix} M_{\mathrm{app}_{12}} & M_{\mathrm{app}_{13}} \\ M_{\mathrm{app}_{42}} & M_{\mathrm{app}_{43}} \end{bmatrix}. \tag{3.35}$$

with

$$M_{\mathrm{app}_{12}} = \frac{k_{\mathrm{eq}.12}}{\omega^2}, M_{\mathrm{app}_{13}} = \frac{k_{\mathrm{eq}.13}}{\omega^2}, M_{\mathrm{app}_{42}} = \frac{k_{\mathrm{eq}.24}}{\omega^2}, \quad and\ M_{\mathrm{app}_{43}} = \frac{k_{\mathrm{eq}.34}}{\omega^2}. \tag{3.36}$$

The $\mathbf{M}_{\mathrm{app}_{jj}}$ is

$$\mathbf{M}_{\mathrm{app}_{ji}} = \begin{bmatrix} M_{\mathrm{app}_{11}} & M_{\mathrm{app}_{14}} \\ M_{\mathrm{app}_{41}} & M_{\mathrm{app}_{44}} \end{bmatrix}. \tag{3.37}$$

with

$$M_{\mathrm{app}_{11}} = m_1 - \frac{k_{\mathrm{eq}.12} + k_{\mathrm{eq}.13} + k_{\mathrm{eq}.14}}{\omega^2}, \quad M_{\mathrm{app}_{44}} = m_4 - \frac{k_{\mathrm{eq}.14} + k_{\mathrm{eq}.24} + k_{\mathrm{eq}.34}}{\omega^2}, \quad and \tag{3.38}$$

$$M_{\mathrm{app}_{14}} = M_{\mathrm{app}_{41}} = \frac{k_{\mathrm{eq}.14}}{\omega^2}.$$

From Eqs. (3.35) and (3.37), $\mathbf{T}_{ij,\mathrm{free}}$ is given as

$$\begin{aligned}\mathbf{T}_{ij,\mathrm{free}} &= -\left(\mathbf{M}_{\mathrm{app}_{ji}}\right)^{-1}\mathbf{M}_{\mathrm{app}_{jj}} \\ &= -\begin{bmatrix} M_{\mathrm{app}_{12}} & M_{\mathrm{app}_{13}} \\ M_{\mathrm{app}_{42}} & M_{\mathrm{app}_{43}} \end{bmatrix}^{-1}\begin{bmatrix} M_{\mathrm{app}_{11}} & M_{\mathrm{app}_{14}} \\ M_{\mathrm{app}_{41}} & M_{\mathrm{app}_{44}} \end{bmatrix}.\end{aligned} \tag{3.39}$$

In other conditions, $\mathbf{M}_{\mathrm{app}_{jj}}$ is changed. The only difference between $\mathbf{M}_{\mathrm{app}_{jj}}$ and $\mathbf{M}_{\mathrm{app}_{jj}.\mathrm{bc}}$ is the existence of $k_{\mathrm{eq}.L}$ and $k_{\mathrm{eq}.R}$.

$$\begin{aligned}\mathbf{T}_{ij,\mathrm{bc}} &= -\left(\mathbf{M}_{\mathrm{app}_{ji}}\right)^{-1}\mathbf{M}_{\mathrm{app}_{jj}.\mathrm{bc}} \\ &= -\begin{bmatrix} M_{\mathrm{app}_{12}} & M_{\mathrm{app}_{13}} \\ M_{\mathrm{app}_{42}} & M_{\mathrm{app}_{43}} \end{bmatrix}^{-1}\begin{bmatrix} M_{\mathrm{app}_{11}} - \dfrac{k_{\mathrm{eq}.L}}{\omega^2} & M_{\mathrm{app}_{14}} \\ M_{\mathrm{app}_{41}} & M_{\mathrm{app}_{44}} - \dfrac{k_{\mathrm{eq}.R}}{\omega^2} \end{bmatrix}.\end{aligned} \tag{3.40}$$

For the condition with mass modification, some masses characterized by m_L and m_R are added to boundary sets.

$$\Delta m_{jj} = \begin{bmatrix} m_L & 0 \\ 0 & m_R \end{bmatrix}. \tag{3.41}$$

m_L and m_R are masses added on the left-hand-side boundary and right-hand-side boundary, respectively. $\mathbf{M}_{\mathrm{app}_{jj}.\mathrm{bcmm}}$ is acquired by adding the delta mass matrix to $\mathbf{M}_{\mathrm{app}_{jj}.\mathrm{bc}}$

$$\mathbf{M}_{\mathrm{app}_{jj}.\mathrm{bcmm}} = \mathbf{M}_{\mathrm{app}_{jj}.\mathrm{bc}} + \Delta m_{jj}. \tag{3.42}$$

and $\mathbf{T}_{ij,\mathrm{bcmm}}$ can be acquired as

$$\mathbf{T}_{ij,\mathrm{bcmm}} = -\left(\mathbf{M}_{\mathrm{app}_{ji}}\right)^{-1}\mathbf{M}_{\mathrm{app}_{jj}.\mathrm{bcmm}} \tag{3.43}$$

$$= -\begin{bmatrix} M_{\mathrm{app}_{12}} & M_{\mathrm{app}_{13}} \\ M_{\mathrm{app}_{42}} & M_{\mathrm{app}_{43}} \end{bmatrix}^{-1} \begin{bmatrix} M_{\mathrm{app}_{11}} - \dfrac{k_{\mathrm{eq}.L}}{\omega^2} + m_L & M_{\mathrm{app}_{14}} \\ M_{\mathrm{app}_{41}} & M_{\mathrm{app}_{44}} - \dfrac{k_{\mathrm{eq}.R}}{\omega^2} + m_R \end{bmatrix}.$$

Finally, by using Eqs. (3.39), (3.40), and (3.43), the BCM can be obtained as

$$\mathbf{BCM} = \begin{bmatrix} k_{\mathrm{eq}.L} & 0 \\ 0 & k_{\mathrm{eq}.R} \end{bmatrix}. \tag{3.44}$$

Therefore, in an MDOF discrete system with multiple boundary properties, the procedure for extracting boundary properties is verified clearly.

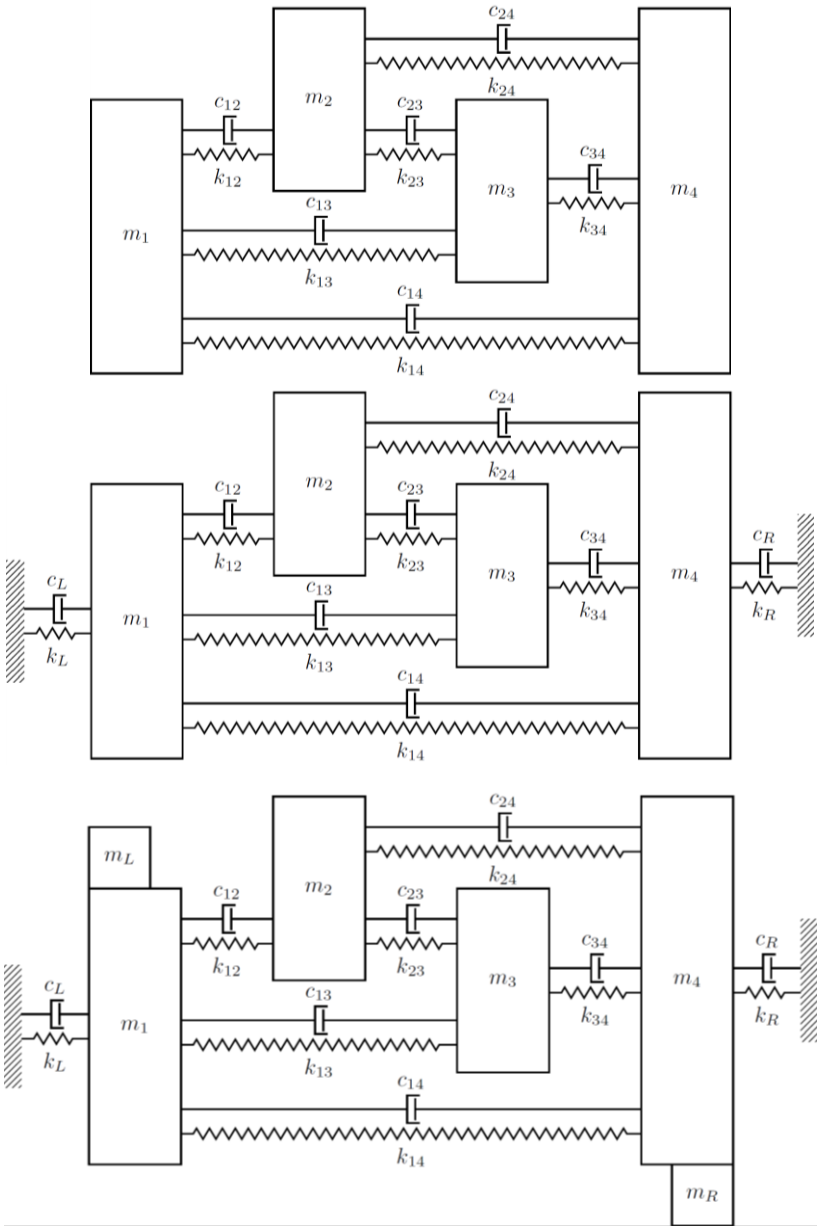

Figure 3.3 4-DOF discrete system: (a) free condition, (b) connected to boundary condition, and (c) connected to boundary condition with mass modification

3.4.3 Finite Beam Model with Multiple Boundary Conditions

In what follows, the proposed method is applied to a finite element beam model, which is the simplest structural form. The numerical beam is simply supported on both sides with stiffness and structural damping. By applying this simple, but not practical, condition, the estimated properties can be easily compared to the exact value directly, which means that the real and imaginary values of the estimated properties represent the stiffness and structural damping, respectively. If they were validated in this condition, the real boundary properties identified from the proposed method might be reliable though the exact value of the boundary properties cannot be found. Fig. 3.4 shows the three boundary conditions applied to the beam structure: free condition (Fig. 3.4(a)), connected to boundary condition (Fig. 3.4(b)) and connected to boundary condition with mass modification (Fig. 3.4(c)). The accelerations at six points are used, including the non-boundary sets i (2, 3, 4, and 5) and boundary sets j (1 and 6) shown in Fig. 3.4. The point number is 1 to 6 from left to right. The properties related to the boundary composed of k_L, k_R, D_L, D_R, m_L, and m_R are shown in Table 3.1. The subscripts L and R are left-hand-side and right-hand-side for coordinates 1 and 6. The additional masses should be a concentrated mass as possible for estimating the boundary properties

appropriately. If the masses are continuous, they could have an effect on the other apparent mass terms in addition to $\mathbf{M}_{\text{app}_{jj}}$ causing inaccurate estimation of properties. The boundary properties estimated from different components are also compared with each other to show that the method is valid in general. A steel beam and aluminum beam having different cross sections are used. The specific properties of the beams are shown in Table 3.2. Only the z-direction accelerations are considered for the simulation.

The equations have to be modified slightly to be applied to the proposed method using only the response acceleration. For this purpose, the transmissibility is derived from the equation of motion using the accelerance,

$$\begin{Bmatrix}\mathbf{a}_i\\ \mathbf{a}_j\end{Bmatrix} = \begin{bmatrix}\mathbf{H}_{ii} & \mathbf{H}_{ij}\\ \mathbf{H}_{ji} & \mathbf{H}_{jj}\end{bmatrix}\begin{Bmatrix}\mathbf{F}_i\\ \mathbf{F}_j\end{Bmatrix}. \tag{3.45}$$

Accelerances, instead of the apparent mass, are used for acquiring the transmissibility, which has to be defined by only the response acceleration data. The accelerations are obtained by substituting $\mathbf{F}_i = \mathbf{1}$. The external force exerted on only the non-boundary sets i and reaction force arise differently according to the boundary model on boundary sets j.

$\mathbf{F}_j = \mathbf{0}$ in the free condition, and therefore, Eq. (3.45) can be changed as

$$\begin{Bmatrix}\mathbf{a}_i\\ \mathbf{a}_j\end{Bmatrix} = \begin{bmatrix}\mathbf{a}_{ii} & \mathbf{a}_{ij}\\ \mathbf{a}_{ji} & \mathbf{a}_{jj}\end{bmatrix}\begin{Bmatrix}\mathbf{1}\\ \mathbf{0}\end{Bmatrix}. \tag{3.46}$$

By using the relationship

$$\mathbf{H}_{ii}\left(\mathbf{H}_{ji}\right)^{+} = \mathbf{a}_{ii}\left(\mathbf{a}_{ji}\right)^{+}, \tag{3.47}$$

the transmissibility can be derived as

$$\begin{aligned}\mathbf{T}_{ij} &= \mathbf{a}_{ii}\left(\mathbf{a}_{ji}\right)^{+} \\ &= -\begin{bmatrix} a_{22} & a_{23} & a_{24} & a_{25} \\ a_{32} & a_{33} & a_{34} & a_{35} \\ a_{42} & a_{43} & a_{44} & a_{45} \\ a_{52} & a_{53} & a_{54} & a_{55} \end{bmatrix}^{-1} \begin{bmatrix} a_{12} & a_{13} & a_{14} & a_{15} \\ a_{62} & a_{63} & a_{64} & a_{65} \end{bmatrix}^{+}.\end{aligned} \tag{3.48}$$

Finally, by using Eq. (3.48), the transmissibility matrices of the component on three different boundary conditions can be estimated.

To confirm whether the results are reliable, the percent errors between the estimated properties and given properties are investigated. The percent error is defined as

$$\%\ \text{Error} = \frac{\text{ExP}_j\left(k_j, D_j\right) - \text{EsP}_j\left(k_j, D_j\right)}{\text{ExP}_j\left(k_j, D_j\right)} \times 100. \tag{3.49}$$

ExP and EsP are the exact properties and estimated properties, respectively. The j coordinate is the boundary set defined at points 1 and 6 that respectively represent the left- and right-hand-sides of the boundary in this case. Specifically, the properties used for checking errors are k_L, D_L, k_R, and D_R.

Fig. 3.5 shows the comparison between the estimated stiffness and the exact stiffness. The results indicating the stiffness estimated from the proposed method are in good agreement with the exact stiffness on both sides, namely, the left and right boundary shown in Fig. 3.5(a) and Fig. 3.5(b), respectively. In keeping with the stiffness estimation results, the estimated structural dampings

shown in Fig. 3.6 are almost the same as the exact structural dampings on both sides. The percentage errors between the estimated and the exact boundary properties are investigated. Fig. 3.7(a) shows that the estimated stiffness gives very high quality results, and the maximum discrepancy is below 1 % on both sides. The structural damping estimation also shows consistent results, as shown in Fig. 3.7(b), and the maximum discrepancy is around 3 % - 4 %. The modified component with the same boundary properties is also used to show that the proposed method performs well. As shown in Figs. 3.8 and 3.9, the estimated properties from different beam structures are almost the same. As a result, the estimation of the boundary properties gives satisfying results in different components.

(a)

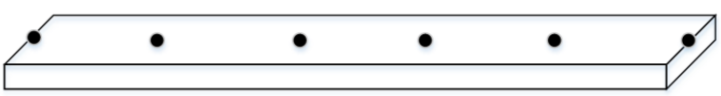

(b)

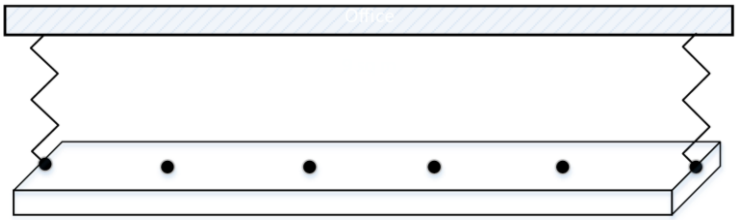

(c)

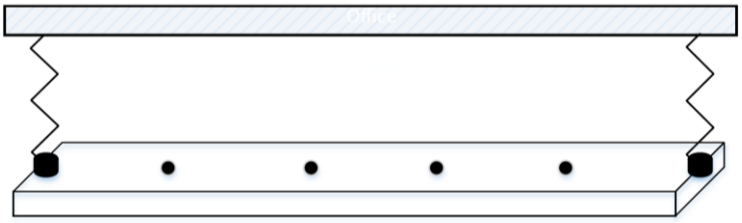

Figure 3.4 Beam structures: (a) free condition, (b) connected to boundary condition, and (c) connected to boundary condition with mass modification

Table 3.1 Boundary properties

	k_L	k_R	D_L	D_R	m_L	m_R
	(N m^{-1})		(N m^{-1})		(kg)	
Free Condition	0	0	0	0	0	0
Connected to b.c	10^6	5×10^6	10^3	5×10^3	0	0
Connected to b.c with m.m	10^6	5×10^6	10^3	5×10^3	1	1

Table 3.2 Component properties

	Original	Modified
Width	0.05	0.07
Height	0.015	0.02
Length	0.5	0.5
Material	Steel	Aluminum
Young's modulus, E $(\mathrm{kg\,m^{-1}\,s^{-2}})$	2.1×10^{11}	7×10^{10}
Poisson's ratio, nu	0.27	0.33
Mass density $(\mathrm{kg\,m^{-3}})$	7850	2712

(a)

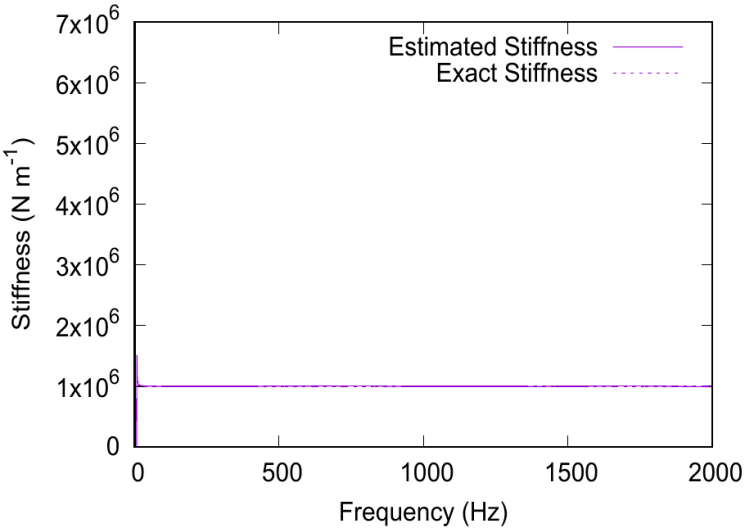

(b)

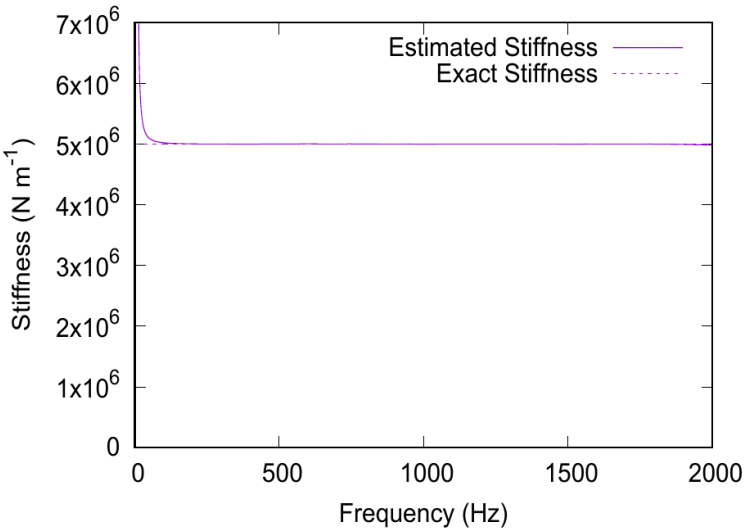

Figure 3.5 Comparison between estimated and exact stiffness of component: (a) on left-hand-side boundary and (b) on right-hand-side boundary

(a)

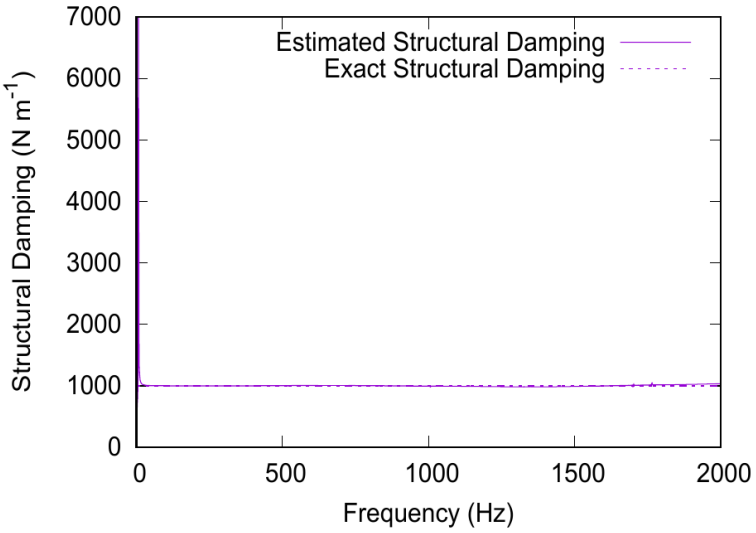

(b)

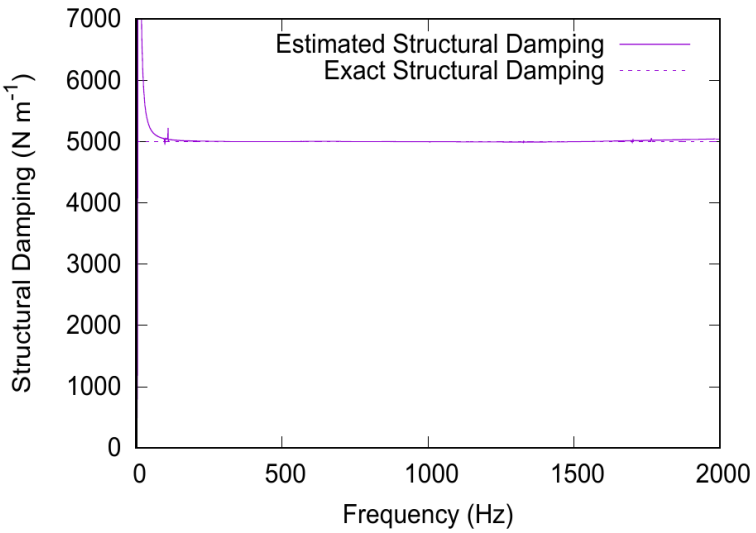

Figure 3.6 Comparison between estimated and exact structural damping of component: (a) on left-hand-side boundary and (b) on right-hand-side boundary

(a)

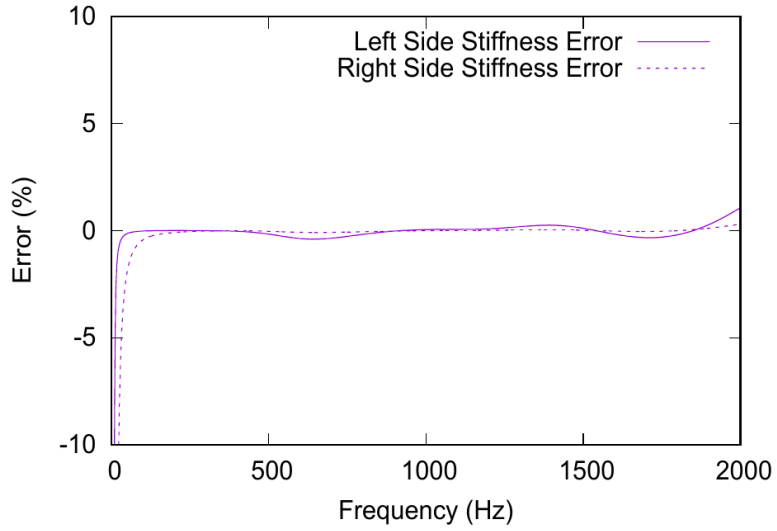

(b)

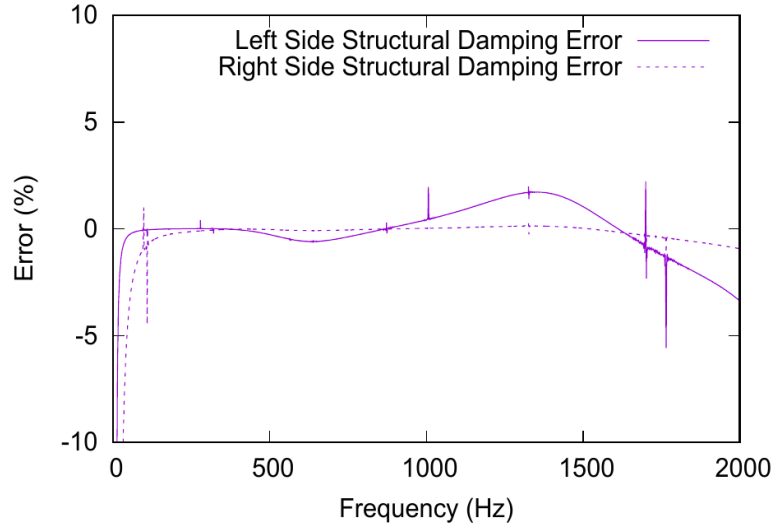

Figure 3.7 Error between estimated and exact boundary properties on both sides:

(a) stiffness and (b) structural damping

(a)

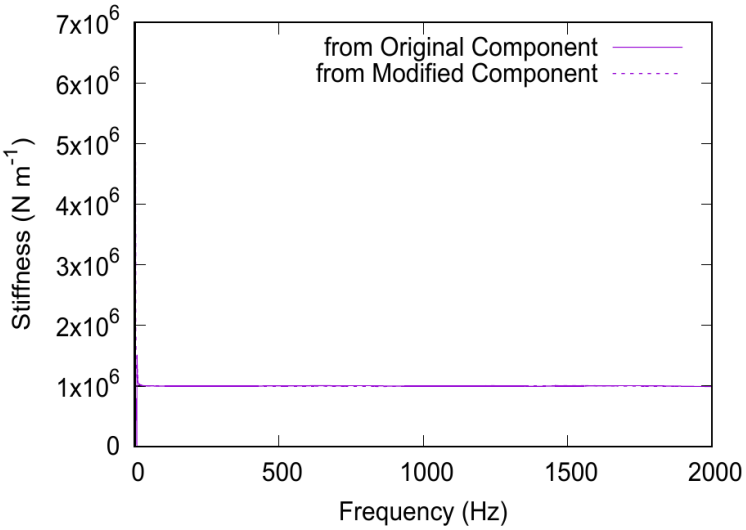

(b)

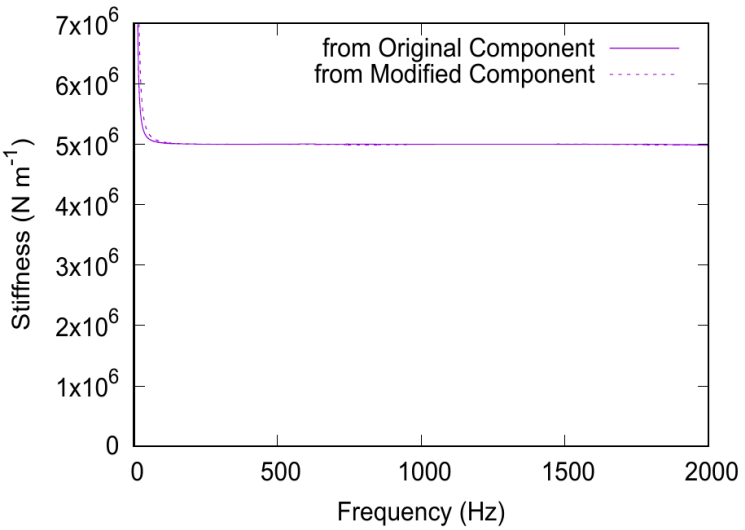

Figure 3.8 Comparison between estimated stiffness from original and modified components: (a) on left-hand-side boundary and (b) on right-hand-side boundary

(a)

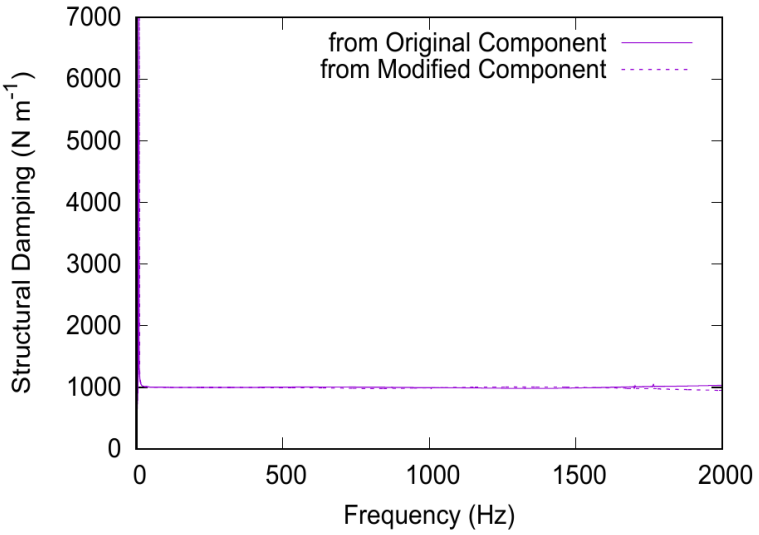

(b)

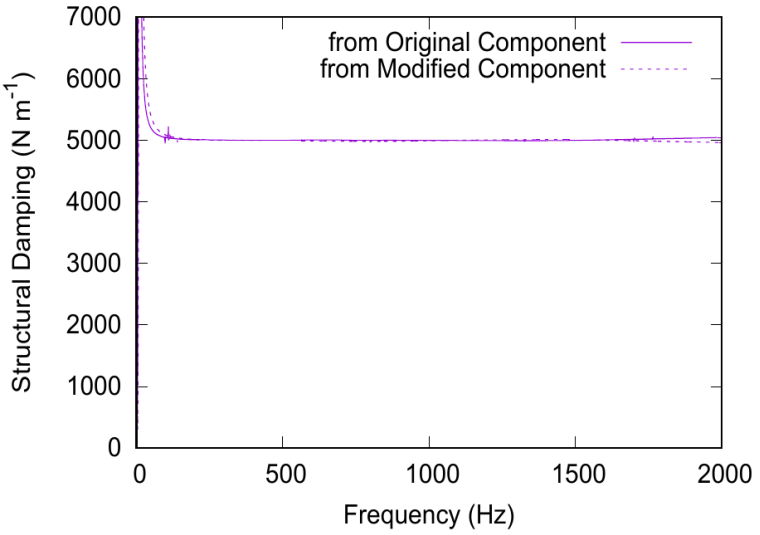

Figure 3.9 Comparison between estimated structural damping from original and modified components: (a) on left-hand-side boundary and (b) on right-hand-side boundary

3.4.4 Effects of the Numbers and Positions of DOFs

For estimating the boundary properties, force should act at least in all of the boundary DOFs. Estimating the boundary properties with the data acquired when force is acting in fewer DOFs than the number of boundary DOFs is similar to solving a single equation composed of multiple variables, namely the equation is indeterminate. Of course, it is possible to estimate the variables using many mathematical techniques of approximation. However, the value estimated using insufficient information is not appropriate for use under practical conditions. Fig. 3.10 shows the difference between the stiffnesses estimated using an incomplete matrix of transmissibility data and a full matrix of transmissibility data. The left-hand-side stiffness is used for explaining the issue in this section. The boundary properties estimated from only a single force are very inaccurate. The Y axis is expressed as a log scale to show the difference between the estimated stiffness from the incomplete and full matrices easily. For this reason, the number of DOFs in which force acts should exceed the number of boundary DOFs. Fig. 3.11 and Fig. 3.12 show the stiffnesses estimated from two input DOFs and three input DOFs, respectively. In Fig. 3.11, the estimated values from two input DOFs are in good agreement with the exact value to some extent, although the result has some errors after 600 Hz when the

input force is acting in positions 2 and 4. Fig. 3.12 shows that the values estimated from three input DOFs are more accurate compared to those from two input DOFs. However, this condition also has errors when positions 2, 4, and 5 are chosen. These results mean that the positions of measuring DOFs are also important for estimating the properties of a continuous structure. The measuring DOFs and their positions have an effect on the reliable frequency range. Fig. 3.13 shows the two stiffnesses estimated from four and six measuring DOFs. The reliable frequency range for the values estimated from six measuring DOFs is clearly wider than that from four measuring DOFs.

In conclusion, at least 4 measuring DOFs, 2 boundary DOFs, and 2 non-boundary DOFs in which force is acting are needed to estimate the boundary properties when the component is connected to two boundary conditions. However, more measuring DOFs and input DOFs will be needed for more accurate results over a wide range of frequencies. Therefore, the number of measuring DOFs and input DOFs should be expanded simultaneously for estimating the properties as accurately as possible, whereas only the number of measuring DOFs should be expanded, while the number of input DOFs are same as the number of boundary conditions, for estimating the properties efficiently.

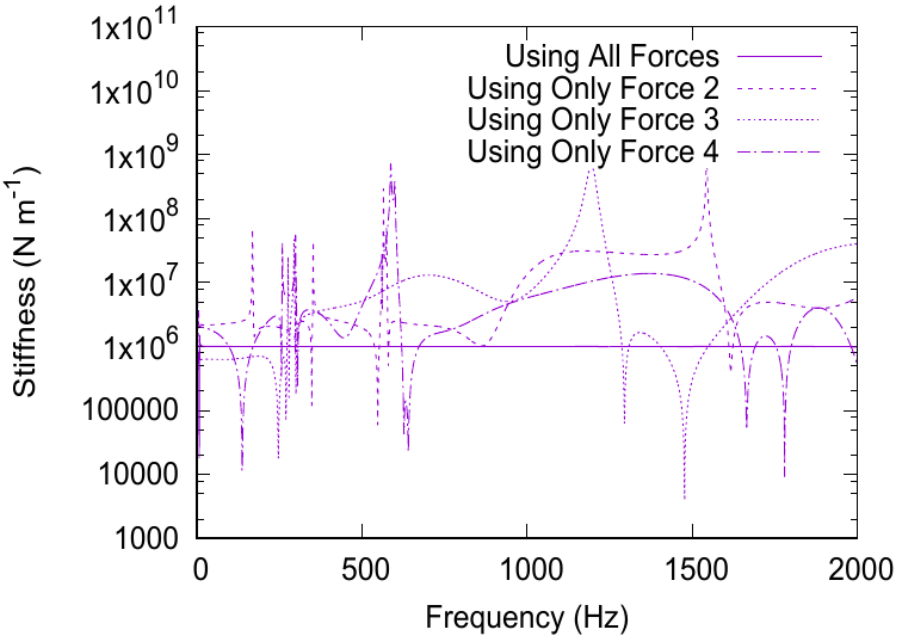

Figure 3.10 Estimated stiffness on left-hand-side boundary using only single input DOF

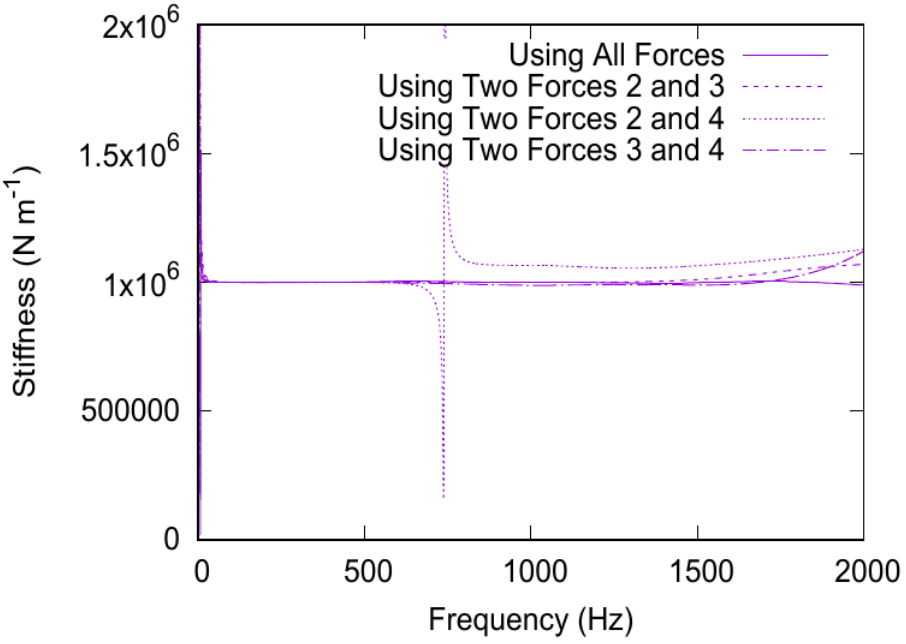

Figure 3.11 Estimated stiffness on left-hand-side boundary using two input DOFs

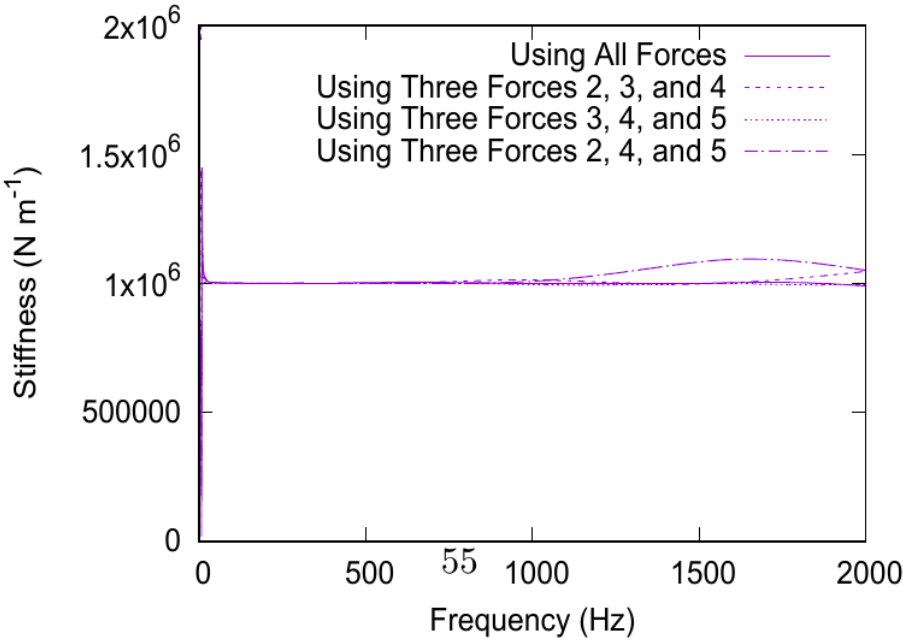

Figure 3.12 Estimated stiffness on left-hand-side boundary using three input DOFs

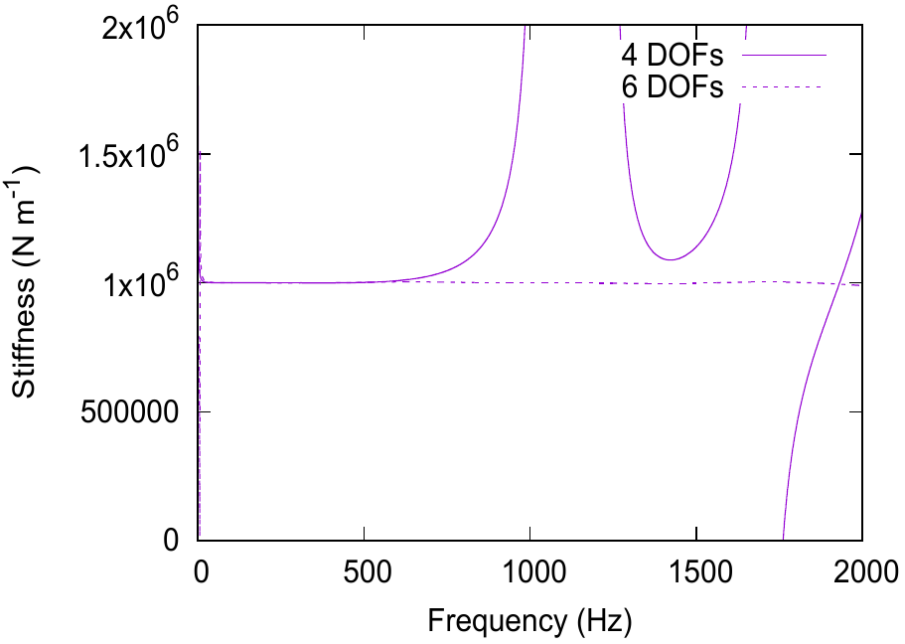

Figure 3.13 Estimated stiffness on left-hand-side boundary using four and six measuring DOFs

3.5 Error Analysis for Assessment of Robustness

3.5.1 Derivation of Error Equation

Because measurement noise always exists under practical conditions, the robustness of the proposed method should be assessed with contaminated data. An equation of estimation error is derived for identifying how the measurement errors affect the estimated property. $\boldsymbol{\alpha}_{ij}$ and $\boldsymbol{\beta}_{ij}$ are used to simplify the derivation.

$$\begin{aligned} \boldsymbol{\alpha}_{ij} &= \mathbf{T}_{ij,\mathrm{bc}} - \mathbf{T}_{ij,\mathrm{bcmm}}, \\ \boldsymbol{\beta}_{ij} &= \mathbf{T}_{ij,\mathrm{free}} - \mathbf{T}_{ij,\mathrm{bc}}. \end{aligned} \tag{3.50}$$

The measurement errors are added to Eq. (3.27).

$$\Delta\mathbf{M}_{\mathrm{app}\,jj} + \boldsymbol{\varepsilon}_{jj,e} = \Delta\mathbf{m}_{jj}\left(\boldsymbol{\alpha}_{ij} + \boldsymbol{\varepsilon}_{ij,\alpha}\right)^{+}\left(\boldsymbol{\beta}_{ij} + \boldsymbol{\varepsilon}_{ij,\beta}\right). \tag{3.51}$$

where $\boldsymbol{\varepsilon}_{jj,e}$, $\boldsymbol{\varepsilon}_{ij,\alpha}$ and $\boldsymbol{\varepsilon}_{ij,\beta}$ are the estimation error, measurement error of $\boldsymbol{\alpha}_{ij}$ and measurement error of $\boldsymbol{\beta}_{ij}$, respectively. Eq. (3.51) is rearranged as

$$\begin{aligned} &\left(\boldsymbol{\alpha}_{ij} + \boldsymbol{\varepsilon}_{ij,\alpha}\right)\left(\Delta\mathbf{m}_{jj}\right)^{-1}\boldsymbol{\varepsilon}_{jj,e} \\ &\qquad = \left(\boldsymbol{\beta}_{ij} + \boldsymbol{\varepsilon}_{ij,\beta}\right) - \left(\boldsymbol{\alpha}_{ij} + \boldsymbol{\varepsilon}_{ij,\alpha}\right)\left(\Delta\mathbf{m}_{jj}\right)^{-1}\Delta\mathbf{M}_{\mathrm{app}\,jj}. \end{aligned} \tag{3.52}$$

$\boldsymbol{\beta}_{ij}$ and $\boldsymbol{\alpha}_{ij}\left(\Delta\mathbf{m}_{jj}\right)^{-1}\Delta\mathbf{M}_{\mathrm{app}\,jj}$ are canceled. Then,

$$\left(\boldsymbol{\alpha}_{ij} + \boldsymbol{\varepsilon}_{ij,\alpha}\right)\left(\Delta\mathbf{m}_{jj}\right)^{-1}\boldsymbol{\varepsilon}_{jj,e} = \boldsymbol{\varepsilon}_{ij,\beta} - \boldsymbol{\varepsilon}_{ij,\alpha}\left(\Delta\mathbf{m}_{jj}\right)^{-1}\Delta\mathbf{M}_{\mathrm{app}\,jj}. \tag{3.53}$$

By substituting $\left(\Delta\mathbf{m}_{jj}\right)^{-1}\Delta\mathbf{M}_{\mathrm{app}_{jj}}$ with $\left(\boldsymbol{\alpha}_{ij}\right)^{+}\boldsymbol{\beta}_{ij}$, the equation is changed to

$$\left(\boldsymbol{\alpha}_{ij}+\boldsymbol{\varepsilon}_{ij,\alpha}\right)\left(\Delta\mathbf{m}_{jj}\right)^{-1}\boldsymbol{\varepsilon}_{jj,e}=\boldsymbol{\varepsilon}_{ij,\beta}-\boldsymbol{\varepsilon}_{ij,\alpha}\left(\boldsymbol{\alpha}_{ij}\right)^{+}\boldsymbol{\beta}_{ij}. \tag{3.54}$$

Thus, the equation of estimation error can be derived.

$$\boldsymbol{\varepsilon}_{jj,e}=\Delta\mathbf{m}_{jj}\left(\boldsymbol{\alpha}_{ij}+\boldsymbol{\varepsilon}_{ij,\alpha}\right)^{+}\left\{\boldsymbol{\varepsilon}_{ij,\beta}\left(\boldsymbol{\beta}_{ij}\right)^{+}-\boldsymbol{\varepsilon}_{ij,\alpha}\left(\boldsymbol{\alpha}_{ij}\right)^{+}\right\}\boldsymbol{\beta}_{ij}. \tag{3.55}$$

$\boldsymbol{\varepsilon}_{ij,\alpha}$ and $\boldsymbol{\varepsilon}_{ij,\beta}$ are errors of $\boldsymbol{\alpha}_{ij}$ and $\boldsymbol{\beta}_{ij}$, respectively.

$$\begin{aligned}\boldsymbol{\varepsilon}_{ij,\alpha}&=\boldsymbol{\varepsilon}_{ij,\mathrm{bc}}-\boldsymbol{\varepsilon}_{ij,\mathrm{bcmm}},\\ \boldsymbol{\varepsilon}_{ij,\beta}&=\boldsymbol{\varepsilon}_{ij,\mathrm{free}}-\boldsymbol{\varepsilon}_{ij,\mathrm{bc}}.\end{aligned} \tag{3.56}$$

Finally, the estimation error is expressed as

$$\begin{aligned}\boldsymbol{\varepsilon}_{jj,e}=\Delta\mathbf{m}_{jj}&\left(\boldsymbol{\alpha}_{ij}+\boldsymbol{\varepsilon}_{ij,\mathrm{bc}}-\boldsymbol{\varepsilon}_{ij,\mathrm{bcmm}}\right)^{+}\left[\boldsymbol{\varepsilon}_{ij,\mathrm{free}}\left(\boldsymbol{\beta}_{ij}\right)^{+}\right.\\ &\left.-\boldsymbol{\varepsilon}_{ij,\mathrm{bc}}\left\{\left(\boldsymbol{\beta}_{ij}\right)^{+}+\left(\boldsymbol{\alpha}_{ij}\right)^{+}\right\}+\boldsymbol{\varepsilon}_{ij,\mathrm{bcmm}}\left(\boldsymbol{\alpha}_{ij}\right)^{+}\right]\boldsymbol{\beta}_{ij}.\end{aligned} \tag{3.57}$$

Fig. 3.14(a) is the estimation error obtained from subtraction of the estimated stiffnesses using noise-free transmissibilities and transmissibilities contaminated with 5 % random noise. Fig. 3.14(b) is the estimation error obtained by solving the equation (Eq. (3.57)) composed of measurement errors. They are almost same as that shown in Fig. 3.15, which shows the difference between errors from subtraction and calculation. The equation of estimation error is well derived. Thus, figuring out how each measurement error affects the estimation error is possible.

(a)

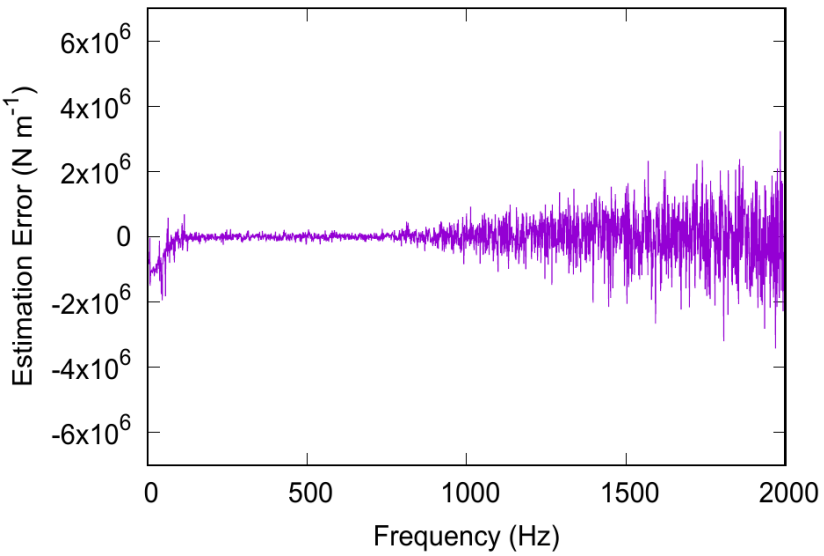

(b)

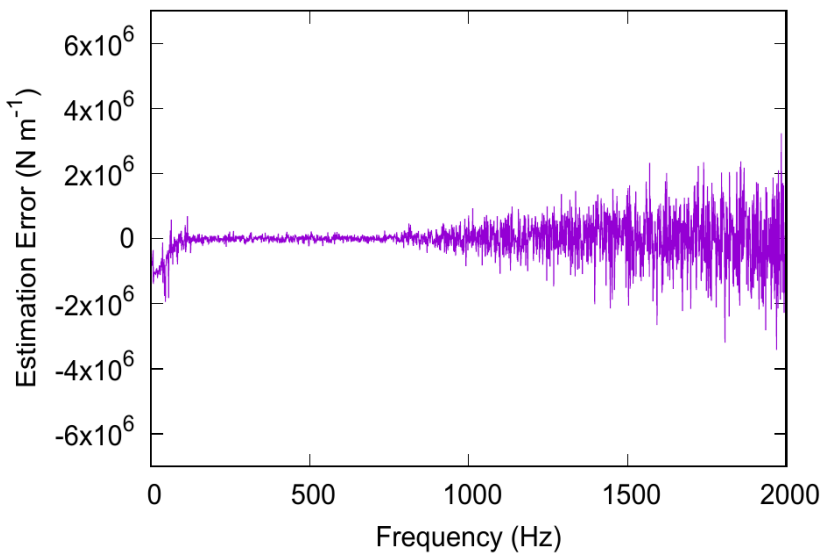

Figure 3.14 Estimation errors: (a) from subtraction and (b) from calculation

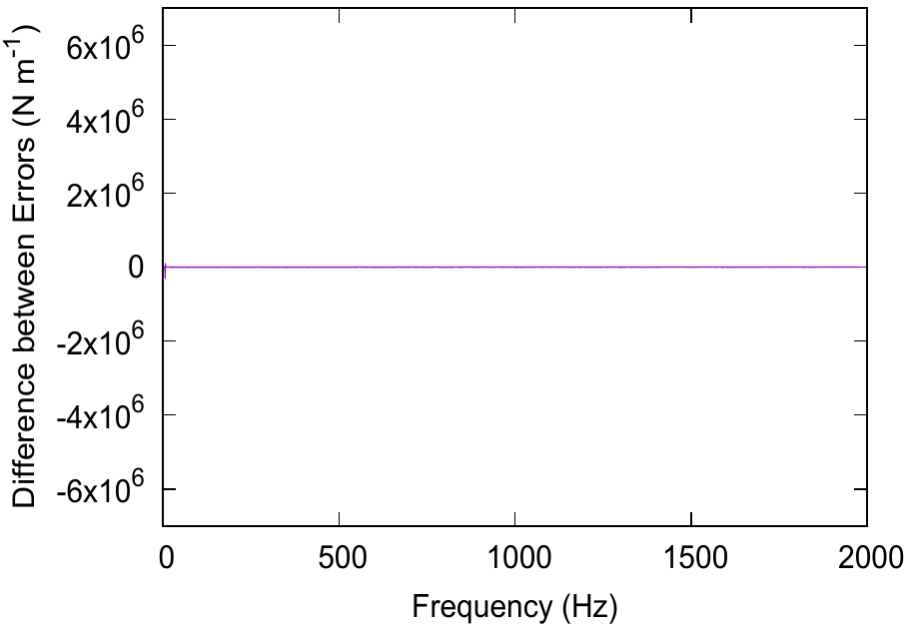

Figure 3.15 Difference between errors from subtraction and from calculation

3.5.2 Effects of Measurement Noise

Transmissibilities contaminated with some normally distributed random noise with a mean value of noise-free transmissibilities and variance of 1 %, 3 % and 5 % of the mean value are used for analyzing the sensitivity of noise effects. Before adding the variety level of noise to the transmissibilities, 1 % and 5 % random noise are used for investigating the noise effect. Fig. 3.16 shows the left-hand-side stiffness estimated from transmissibilities contaminated with 1 % noise. Fig. 3.17 shows the estimated left-hand-side stiffness from the transmissibilities contaminated with 5 % random noise. The effect of random noise is shown. It is obvious that the noise effect is amplified as the frequency range is increased because the boundary properties are estimated from acceleration data. It seems that the distributed random noise is amplified based on the exact property, as shown in Fig. 3.16 and Fig. 3.17. The error of estimated stiffness from the 5 % noisy transmissibilities is larger than that from the 1 % noisy transmissibilities. If the noise of α_{ij} is smaller than α_{ij} in Eq. (3.57), the estimation error is expressed as a linear combination of transmissibility noises. Thus, the noise level in Fig. 3.17 is about 5 times that in Fig. 3.16.

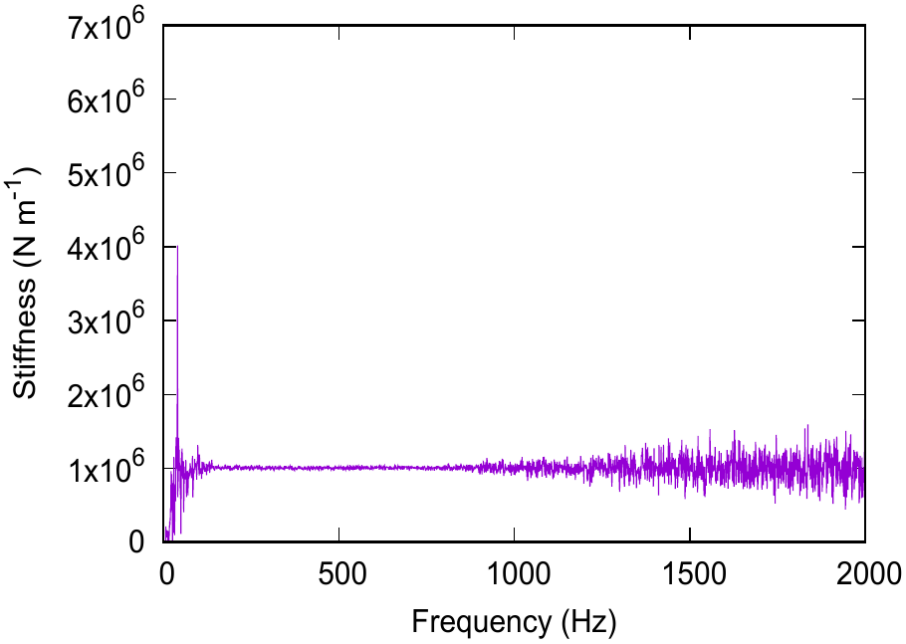

Figure 3.16 Estimated stiffness on left-hand-side boundary using transmissibilities contaminated by 1 % noise

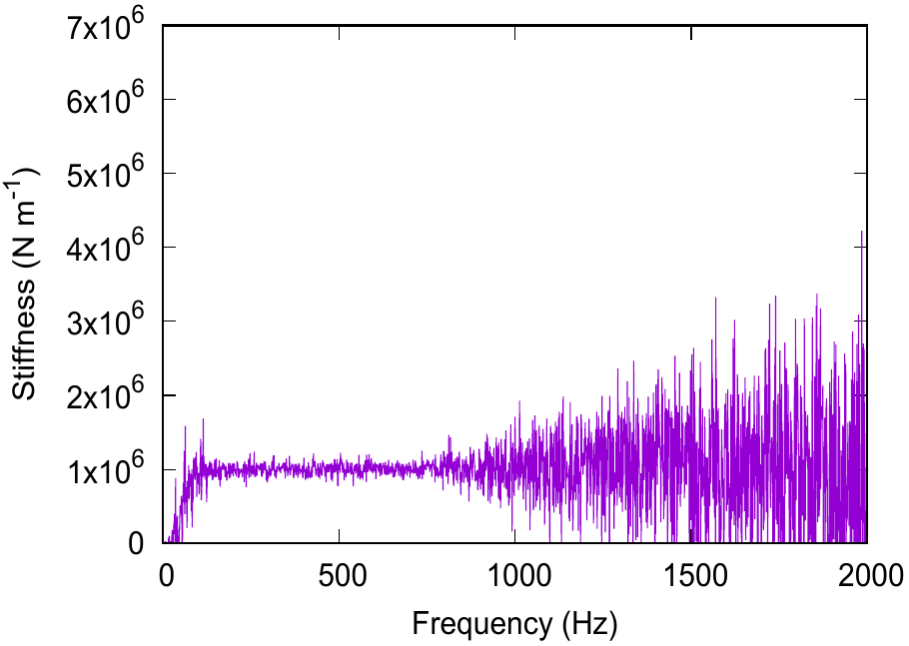

Figure 3.17 Estimated stiffness on left-hand-side boundary using transmissibilities contaminated by 5 % noise

3.5.3 Comparison of Estimated Properties with and without Measurement noise

The estimated property contaminated with measurement noise cannot be used as is. Thus, the curves should first be smoothed to minimize the noise effect, and should then be compared with the exact property for assessing whether the estimated value is usable. Fig. 3.18 and Fig. 3.19 show the estimated stiffness and the structural damping, respectively, on both sides with contaminated transmissibilities after smoothing the curves. The estimated properties on both sides seem to agree well with the exact properties. However, errors increase as the noise level increases in the lower frequency range. Specifically, errors of the right-hand-side properties shown in Fig. 3.18(a) and Fig. 3.19(a) are larger than those of the left-hand-side properties shown in Fig. 3.18(b) and Fig. 3.19(b). The proposed method uses the transmissibilities under three different conditions. In Eq. (3.27), because $\mathrm{T}_{ij,\mathrm{bc}}$ and $\mathrm{T}_{ij,\mathrm{bcmm}}$ are not very different in the lower frequency range where the effect of mass is small, accurate transmissibilities are needed for estimating the boundary properties accurately. For this reason, the properties are not estimated well in the lower frequency range even though the transmissibilities have a low level of noise. Of course, the accuracy can be improved by using the stiffness modification

technique or a heavier mass. However, use of the stiffness modification technique is not possible under practical conditions and increasing the mass has a limitation. The errors of the right-hand-side stiffness are larger than those of the left-hand-side stiffness at lower frequencies because identical 1 kg masses are used for estimating the boundary properties even though the right-hand-side boundary properties are 5 times higher than the left-hand-side boundary properties. Under these conditions, the left-hand-side boundary properties can be estimated more accurately than the right-hand-side-boundary properties. Increasing the mass on the right-hand-side boundary could give improved results for the right-hand-side boundary properties. Thus, errors in the lower frequency range should be considered before using the proposed method.

(a)

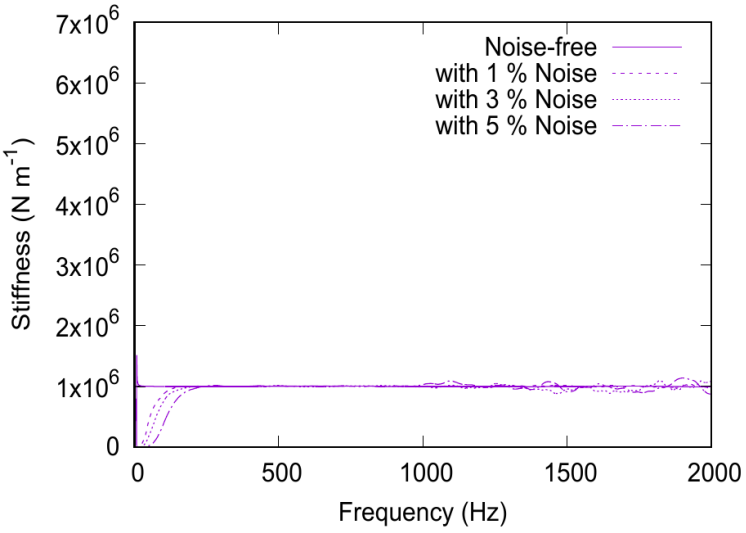

(b)

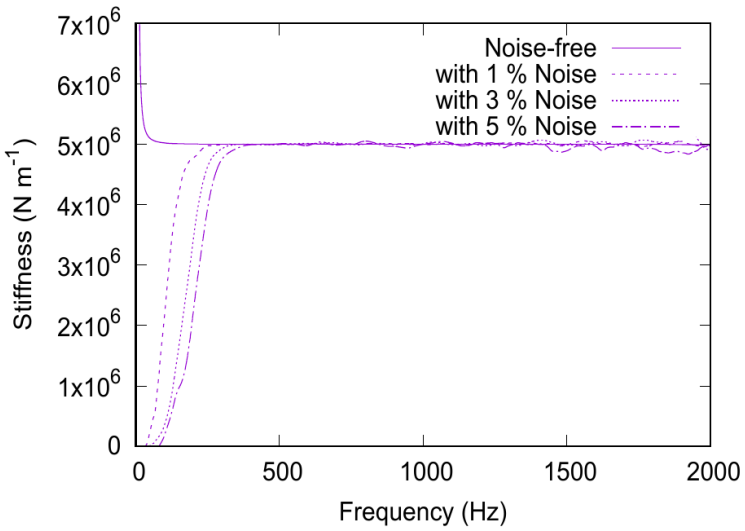

Figure 3.18 Estimated stiffness with polluted transmissibilities: (a) on left-hand-side boundary after smoothing and (b) on right-hand-side boundary after smoothing

(a)

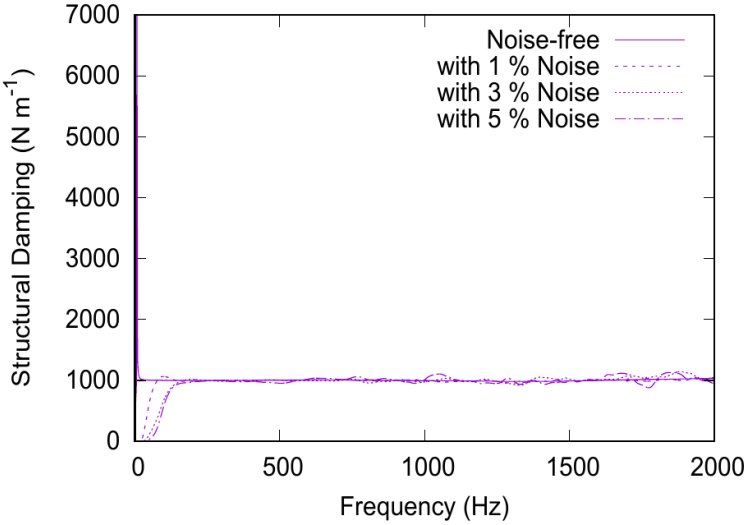

(b)

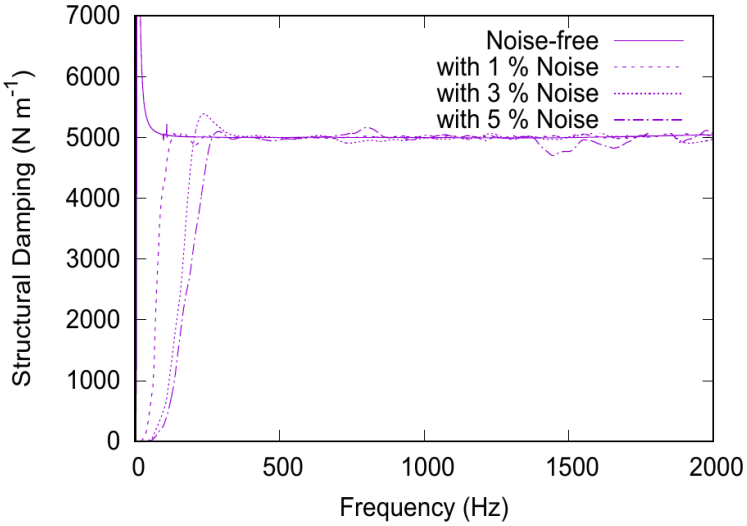

Figure 3.19 Estimated structural damping with polluted transmissibilities: (a) on left-hand-side boundary after smoothing and (b) on right-hand-side boundary after smoothing

3.5.4 Comparison of Estimation Errors with and without Measurement noise

Fig. 3.20 and Fig. 3.21 show the estimation errors of stiffness and structural damping, respectively, on both sides with contaminated transmissibilities after smoothing the curves. The error tends to increase as the noise level increases even though the curves are smoothed. Fig. 3.20(b) supports the hypothesis of the proposed method that the right-hand-side stiffness is estimated well with about 5 % error of maximum discrepancy. Fig. 3.20(a) shows that the errors of right-hand-side stiffness look larger than those of left-hand-side stiffness. However, the maximum discrepancy of estimation error is about 10 %, which can be considered a satisfactory result. The estimation errors of structural damping in Fig. 3.21 show the same tendencies as Fig. 3.20. In conclusion, after exponential smoothing, the estimated properties on both sides give fairly reliable results over a wide frequency range.

(a)

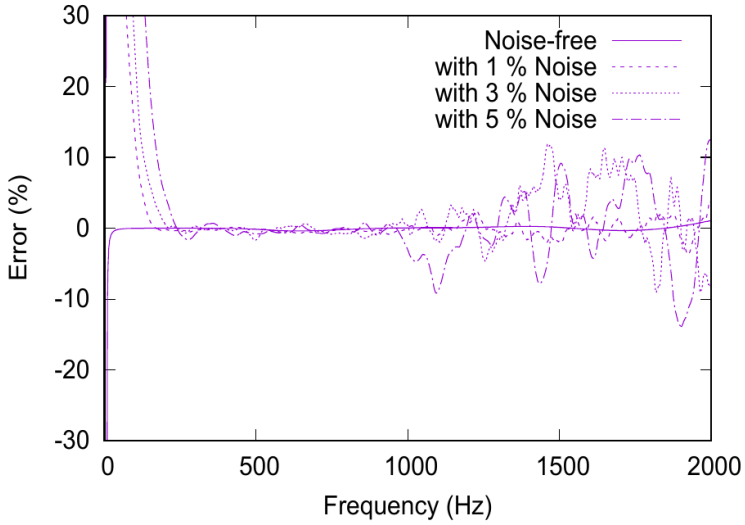

(b)

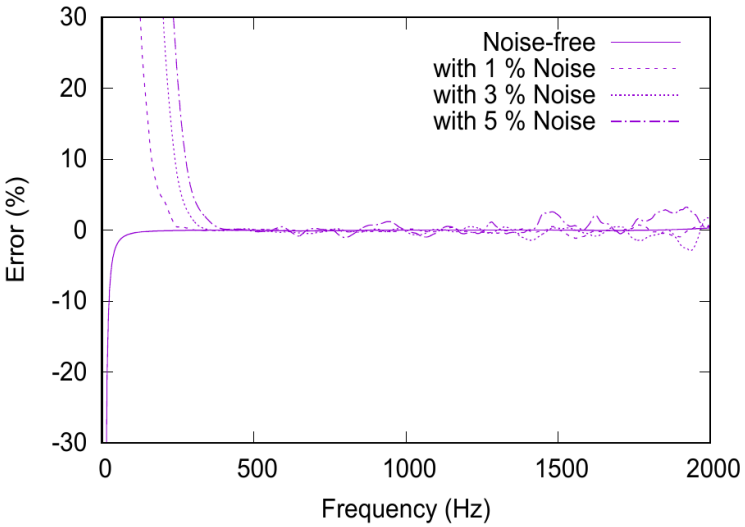

Figure 3.20 Errors between estimated and exact stiffness on both sides: (a) left-hand-side stiffness after smoothing and (b) right-hand-side stiffness after smoothing

(a)

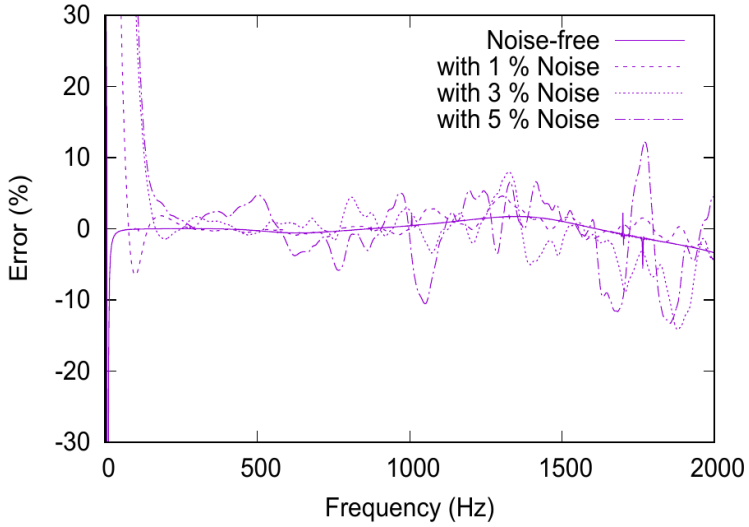

(b)

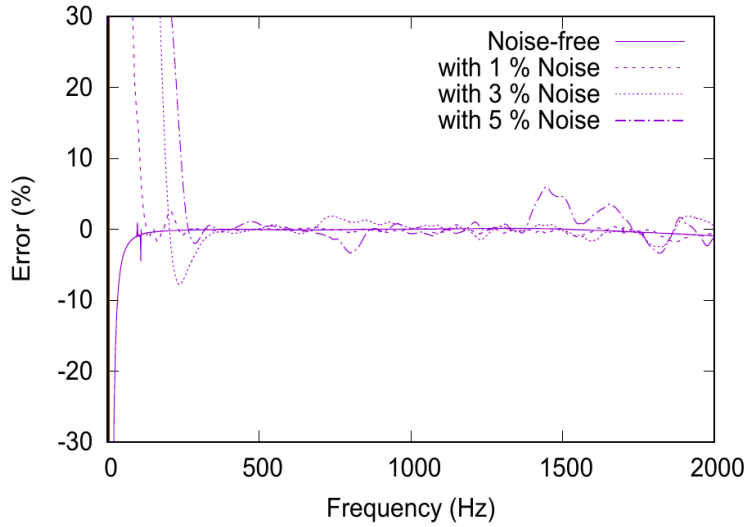

Figure 3.21 Errors between estimated and exact structural damping on both sides: (a) left-hand-side structural damping after smoothing and (b) right-hand-side structural damping after smoothing

3.6 Summary and Conclusion

In this Chapter, a new methodology for using the transmissibility for identifying the boundary properties is proposed. This method differs from all previous studies that use FRFs for property estimation. The transmissibilities acquired from the component under three different conditions are used for defining the relation. In many practical cases, the force cannot be measured easily because the components constituting the entire system are assembled compactly. By using only the response data, the effects caused by incorrectly measured forces exerted on the component connected to the entire system could be reduced. This could be applied to all components connected to any boundary systems as far as sensors can be installed.

This method is validated numerically using discrete and continuous models. A 2-DOF discrete system with a single boundary condition and a 4-DOF discrete system with multiple boundary conditions are adopted to verify the proposed method. In both discrete models, the boundary properties are extracted exactly. This method is also validated with a beam model, which is a continuous system with the simplest structural form. For comparing the exact properties and estimated properties directly, the stiffness and structural damping are given as boundary properties. This means that the real values and

imaginary values of the estimated properties represent the stiffness and structural damping, respectively. The results indicated that the method is still valid in a continuous model system. Furthermore, the robustness of the method is investigated by assessing how the estimation error is affected by measurement noise of contaminated transmissibilities. The properties estimated with noisy data still give satisfactory results after smoothing the curves. Overall, this study shows that the proposed methodology is fully reliable, and it can be expected to contribute to research and development by being used for identifying the boundary properties and by being applied to components in the early design phase before producing a real component.

CHAPTER 4

RELATIVE SENSITIVITY ANALYSIS

4.1 Introduction

The primary purpose of the work described in this Chapter is to suggest sensitivity indices expressed by transmissibility for relative sensitivity analysis of responses. Recently, Kim et al. [58] proposed a new approach for sensitivity analysis that can indicate the proper location for design modification using only the response data, without identifying the system characteristics under intact conditions. They used the transmissibility concept to derive the equation. They used only the output data to derive the equation for the nodal sensitivity, without system identification. However, the derived equation is applicable only to the mass variable. In addition, it was assumed that the response variation of the reference node with respect to a small mass modification applied to node i is small enough to be ignored. This indicates that the crosstalk was not considered. In practical situations, the mass modification at specific node has an effect on the response at the other nodes according to characteristics of frequency response functions because mass variation could be considered as force

variation. Therefore, crosstalk should be considered while indicating the location where the design modification needs to be applied for obtaining more reasonable information.

The present study does not merely adopt the transmissibility concept to calculate the relative sensitivity, but also considers the crosstalk effects between nodes. The indices, including the crosstalk effects, could give meaningful information about the relative sensitivity of the responses. Two types of indices related to each variable are proposed: sensitivity indices of the response for positions of variables, and the sensitivity indices of responses for positions of responses. The former indicates the appropriate position where the design variable could be modified, while the latter indicates the effect of a specific design variable on the responses. These indices are applicable for mass, stiffness, and damping. The proposed indices were analytically and numerically investigated to determine whether they adequately reflect the relative changes in response to small design modifications. The analytical model of a 7-DOF discrete system and two numerical beam models were used for verification and application examples.

4.2 Sensitivity Indices

In this Chapter, sensitivity indices are proposed to analyze the relative sensitivity characteristics of responses using transmissibility. The purpose is to indicate sensitive position in a component with respect to design variables in a specific position only using response data.

A general system composed of three different coordinates is considered as shown in Fig. 4.1. An external force is applied to the i coordinate, and a small design modification is applied to the j coordinate. The target set is indicated as the t coordinate. The equation of motion using the apparent mass ($\mathbf{M}_{\text{app}}$) and acceleration is

$$\mathbf{M}_{\text{app}}\mathbf{a} = \mathbf{F}. \tag{4.1}$$

The apparent mass is expressed as

$$\mathbf{M}_{\text{app}} = \left(\mathbf{M} - \frac{\mathbf{K} + \text{j}\omega\mathbf{C}}{\omega^2}\right), \tag{4.2}$$

where $\mathbf{M}$, $\mathbf{C}$, $\mathbf{K}$, ω, $\mathbf{a}$, and $\mathbf{F}$ denote the mass, viscous damping, stiffness, angular frequency, acceleration, and force, respectively. A direct differentiation method is applied to Eq. (4.1) to derive the response sensitivity as follows:

$$\frac{\partial \mathbf{M}_{\text{app}}}{\partial v_j}\mathbf{a} + \mathbf{M}_{\text{app}}\frac{\partial \mathbf{a}}{\partial v_j} = \frac{\partial \mathbf{F}}{\partial v_j}. \tag{4.3}$$

Eq. (4.3) can be rearranged using the accelerance matrix $\mathbf{H}$ as follows:

$$\frac{\partial \mathbf{a}}{\partial v_j} = \mathbf{H}\left(\frac{\partial \mathbf{F}}{\partial v_j} - \frac{\partial \mathbf{M}_{\text{app}}}{\partial v_j}\mathbf{a}\right). \tag{4.4}$$

All apparent masses and external forces except for $\mathbf{M}_{\text{app}}{}_{jj}$ are excluded because small design modifications are only applied to the j coordinate. Hence, the equation is changed as follows:

$$\begin{Bmatrix} \frac{\partial \mathbf{a}_i}{\partial v_j} \\ \frac{\partial \mathbf{a}_j}{\partial v_j} \\ \frac{\partial \mathbf{a}_t}{\partial v_j} \end{Bmatrix} = \begin{bmatrix} \mathbf{H}_{ii} & \mathbf{H}_{ij} & \mathbf{H}_{it} \\ \mathbf{H}_{ji} & \mathbf{H}_{jj} & \mathbf{H}_{jt} \\ \mathbf{H}_{ti} & \mathbf{H}_{tj} & \mathbf{H}_{tt} \end{bmatrix} \begin{Bmatrix} \mathbf{0} \\ -\frac{\partial \mathbf{M}_{\text{app}}}{\partial v_j}\mathbf{a}_j \\ \mathbf{0} \end{Bmatrix}. \tag{4.5}$$

In Eq. (4.5), $-\frac{\partial \mathbf{M}_{\text{app}}}{\partial v_j}\mathbf{a}_j$ can be considered an infinitesimal added force resulting from the design variables. Consequently, response sensitivities to the design variables can be obtained by using the infinitesimal added force produced by design modifications and accelerances of the system:

$$\begin{aligned} \frac{\partial \mathbf{a}_i}{\partial v_j} &= \mathbf{H}_{ij}\left(-\frac{\partial \mathbf{M}_{\text{app}}}{\partial v_j}\mathbf{a}_j\right), \\ \frac{\partial \mathbf{a}_j}{\partial v_j} &= \mathbf{H}_{jj}\left(-\frac{\partial \mathbf{M}_{\text{app}}}{\partial v_j}\mathbf{a}_j\right), \\ \frac{\partial \mathbf{a}_t}{\partial v_j} &= \mathbf{H}_{tj}\left(-\frac{\partial \mathbf{M}_{\text{app}}}{\partial v_j}\mathbf{a}_j\right). \end{aligned} \tag{4.6}$$

The derivative of the apparent masses to the design variable and the responses play a role as an added infinitesimal force. Response sensitivities are expressed by this force and accelerance. Hence, a small design modification generates the

force that results in changes in the responses in a component. The accelerances should be known to obtain the exact value of response sensitivity. However, relative sensitivity of responses can be analyzed by introducing a sensitivity index based on the transmissibility concept that does not require an input force. The general form of sensitivity index can be defined as follows:

$$\textbf{Sensitivity Index} = \frac{S_k}{\sum_{i=1}^{n} S_i}. \tag{4.7}$$

S_k is a sensitivity of response at position k with respect to variable. The nodes influencing response sensitivity are different based on the type of variable. Response sensitivities are affected by a single node when a design variable corresponds to a mass, and by two nodes connected to each other when the design variables correspond to stiffness and damping.

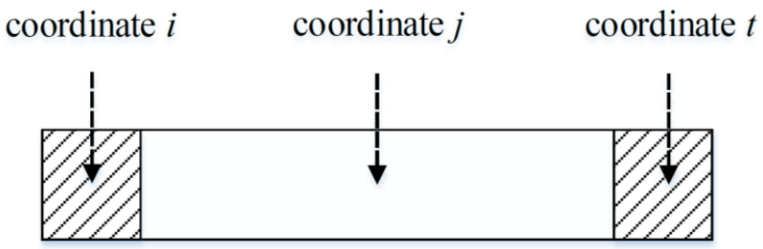

Figure 4.1 Schematic model of system

4.2.1 Sensitivity Indices with respect to Mass

4.2.1.1 Sensitivity Index for Positions of Variable: $\mathbf{SI}(m_i, r_k)$

$$\mathrm{SI}(m_i, r_k) = \frac{H_{ki} a_i}{\sum_{j=1}^{n} H_{kj} a_j}. \tag{4.8}$$

$\mathrm{SI}(m_i, r_k)$ is the sensitivity index of a response at node k with respect to the mass at node i, and is used to identify the sensitive position at which a small mass modification can be applied. By using the reciprocity theorem, the equation is changed as follows:

$$\mathrm{SI}(m_i, r_k) = \frac{a_i}{\sum_{j=1}^{n} T_{ji,f_k} a_j}, \tag{4.9}$$

where T_{ji,f_k} and a_i denote the transmissibility from node i to node j when the external force is applied to node k and the response in operational conditions, respectively. The sensitivity index can be simply expressed by transmissibilities as follows:

$$\mathrm{SI}(m_i, r_k) = \frac{1}{\sum_{j=1}^{n} T_{ji,f_k} T_{ji,f_s}}. \tag{4.10}$$

In Eq. (4.10), f_s denotes the operating force of a source acting on a specific node. The specific node where the external force acts can be varied based on system assembly.

4.2.1.2 Sensitivity Index for Positions of Response: $\mathbf{SI}(m_k, r_i)$

$$\mathrm{SI}(m_k, r_i) = \frac{H_{ik} a_k}{\sum_{j=1}^{n} H_{jk} a_k}. \tag{4.11}$$

$\mathrm{SI}(m_k, r_i)$ denotes sensitivity index of the response at node i with respect to the mass at node k for analyzing the manner in which the responses are mostly affected by a small mass modification. It should be noted that a_k, which corresponds to the operating acceleration at the node where the design variable was modified, is excluded. The sensitivity index is simply expressed by transmissibility as follows:

$$\mathrm{SI}(m_k, r_i) = \frac{1}{\sum_{j=1}^{n} T_{ji,f_k}}. \tag{4.12}$$

The $\mathrm{SI}(m_k, r_i)$ is independent of the source.

4.2.2 Sensitivity Indices with respect to Stiffness

4.2.2.1 Sensitivity Index for positions of variable: $\mathbf{SI}(k_{ij}, r_k)$

$$\mathrm{SI}(k_{ij}, r_k) = \frac{H_{ki}\left(-\frac{1}{\omega^2}\right)(a_i - a_j) - H_{kj}\left(-\frac{1}{\omega^2}\right)(a_i - a_j)}{\sum_{r=1}^{n-1}\sum_{s=r+1}^{n}\left\{H_{kr}\left(-\frac{1}{\omega^2}\right)(a_r - a_s) - H_{ks}\left(-\frac{1}{\omega^2}\right)(a_r - a_s)\right\}}. \quad (4.13)$$

$\mathrm{SI}(k_{ij}, r_k)$ corresponds to the sensitivity index of the response at node k with respect to stiffness between node i and node j to identify the sensitive position at which the small stiffness modification can be applied. Infinitesimal force is a result of the difference in acceleration between two nodes (node i and j) connected to each other by stiffness. There is no resultant force when the stiffness between node i and node j does not exist. Thus, it is necessary to calculate $H_{ki}\left(-\frac{1}{\omega^2}\right)(a_i - a_j) - H_{kj}\left(-\frac{1}{\omega^2}\right)(a_i - a_j)$ only when the stiffness exists.

By using reciprocity theorem, Eq. (4.13) can be rewritten as follows:

$$\mathrm{SI}(k_{ij}, r_k) = \frac{(H_{ik} - H_{jk})(a_i - a_j)}{\sum_{r=1}^{n-1}\sum_{s=r+1}^{n}(H_{rk} - H_{sk})(a_r - a_s)}. \quad (4.14)$$

Eq. (4.14) can be expressed by transmissibility using ${H_{kk}}^{-1}$ as follows:

$$\mathrm{SI}(k_{ij}, r_k) = \frac{(T_{ik,f_k} - T_{jk,f_k})(a_i - a_j)}{\sum_{r=1}^{n-1}\sum_{s=r+1}^{n}(T_{rk,f_k} - T_{sk,f_k})(a_r - a_s)}. \quad (4.15)$$

where a_i and a_j denote responses at operational conditions. Thus, the sensitivity index can be simply expressed using transmissibilities as follows:

$$\mathrm{SI}(k_{ij}, r_k) = \frac{(T_{ik,f_k} - T_{jk,f_k})(1 - T_{ji,f_s})}{\sum_{r=1}^{n-1}\sum_{s=r+1}^{n}(T_{rk,f_k} - T_{sk,f_k})(T_{ri,f_s} - T_{si,f_s})}. \quad (4.16)$$

4.2.2.2 Sensitivity Index for positions of response: $\mathrm{SI}(k_{kl}, r_i)$

$$\mathrm{SI}(k_{kl}, r_i) = \frac{H_{ik}\left(-\frac{1}{\omega^2}\right)(a_k - a_l) - H_{il}\left(-\frac{1}{\omega^2}\right)(a_k - a_l)}{\sum_{j=1}^{n}\left\{H_{jk}\left(-\frac{1}{\omega^2}\right)(a_k - a_l) - H_{jl}\left(-\frac{1}{\omega^2}\right)(a_k - a_l)\right\}}. \quad (4.17)$$

$\mathrm{SI}(k_{kl}, r_i)$ denotes the sensitivity index of response at node i with respect to stiffness between node k and node l for analyzing the manner in which the responses are affected by the small stiffness modification. The acceleration effect is excluded in this case and the equation is simplified as follows:

$$\mathrm{SI}(k_{kl}, r_i) = \frac{H_{ik} - H_{il}}{\sum_{j=1}^{n}(H_{jk} - H_{jl})}. \quad (4.18)$$

However, the index cannot be easily expressed by transmissibility because the equation is composed of FRFs, H_{ik} and H_{il}, which require the application of input forces to different positions. Thus, it is necessary to slightly modify the equation by using a mathematical technique to express the index by transmissibility. The sensitivity index related to stiffness can be redefined after

modifying the numerator of the index by multiplying the inverse of the driving point inertance at node k. This is expressed as follows:

$$(H_{ik} - H_{il}){H_{kk}}^{-1} = T_{ik,f_k} - H_{il}{H_{kk}}^{-1}. \quad (4.19)$$

The second term on the right-hand side of Eq. (4.19) can be modified using ${H_{kl}}^{-1}H_{kl}$ as follows:

$$T_{ik,f_k} - H_{il}{H_{kl}}^{-1}H_{kl}{H_{kk}}^{-1} = T_{ik,f_k} - T_{ik,f_l}H_{kl}{H_{kk}}^{-1}. \quad (4.20)$$

H_{kl} in Eq. (4.20) can be changed as H_{lk} by using the reciprocity theorem, and thus the equation is expressed as follows:

$$(H_{ik} - H_{il}){H_{kk}}^{-1} = T_{ik,f_k} - T_{ik,f_l}T_{lk,f_k}. \quad (4.21)$$

Although Eq. (4.21) also required the application of input forces to different positions, the information regarding forces does not need to be known because the equation was expressed in terms of transmissibilities. Finally, the index is redefined as follows:

$$\mathrm{SI}(k_{kl}, r_i) = \frac{\left(T_{ik,f_k} - T_{ik,f_l}T_{lk,f_k}\right)}{\sum_{j=1}^{n}\left(T_{jk,f_k} - T_{jk,f_l}T_{lk,f_k}\right)}. \quad (4.22)$$

4.2.3 Sensitivity Indices with respect to Damping

The process to obtain the index related to damping is identical to that for obtaining the index related to stiffness except for the derivative of apparent mass. Therefore, the sensitivity indices with respect to damping are also the same as those with respect to stiffness.

4.2.3.1 Sensitivity Index for positions of variable: $\mathbf{SI}(\boldsymbol{c_{ij}, r_k})$

$$\mathrm{SI}(c_{ij}, r_k) = \frac{\left(T_{ik,f_k} - T_{jk,f_k}\right)\left(1 - T_{ji,f_s}\right)}{\sum_{r=1}^{n-1}\sum_{s=r+1}^{n}\left(T_{rk,f_k} - T_{sk,f_k}\right)\left(T_{ri,f_s} - T_{si,f_s}\right)}. \tag{4.23}$$

4.2.3.2 Sensitivity Index for positions of response: $\mathbf{SI}(\boldsymbol{c_{kl}, r_i})$

$$\mathrm{SI}(k_{kl}, r_i) = \frac{\left(T_{ik,f_k} - T_{ik,f_l}T_{lk,f_k}\right)}{\sum_{j=1}^{n}\left(T_{jk,f_k} - T_{jk,f_l}T_{lk,f_k}\right)}. \tag{4.24}$$

4.3 Verification and Application Examples

4.3.1 MDOF discrete model

The proposed indices are verified by using a one-dimensional 7-DOF discrete model as shown in Fig. 4.2. The system is assembled by springs and dampers with the system parameter properties as shown in Table 4.1. Normalized response variations (NRVs), when the external force is assumed as a unit force acting on node 1 (m_1), are adopted as indicators to verify the proposed sensitivity indices. The four types of NRVs are defined as follows:

$$\begin{aligned}
\mathrm{NRV}(m_i, r_k) &= \frac{\Delta a_k(m_i)}{\sum_{j=1}^{n} \Delta a_k(m_j)}, \\
\mathrm{NRV}(m_k, r_i) &= \frac{\Delta a_i(m_k)}{\sum_{j=1}^{n} \Delta a_j(m_k)}, \\
\mathrm{NRV}(k_{ij}, r_k) &= \frac{\Delta a_k(k_{ij})}{\sum_{r=1}^{n-1} \sum_{s=r+1}^{n} \Delta a_k(k_{rs})}, \\
\mathrm{NRV}(k_{kl}, r_i) &= \frac{\Delta a_i(k_{kl})}{\sum_{j=1}^{n} \Delta a_j(k_{kl})}.
\end{aligned} \tag{4.25}$$

Additionally, 0.01 kg mass and 15,000 N/m stiffness are added to the MDOF model for small design modifications. Fig. 4.3 shows the sensitivity indices and normalized response variations that represent $\mathrm{SI}(m_i, r_2)$, and $\mathrm{NRV}(m_i, r_2)$, respectively. Specifically, 0.01 kg mass is added on node 1 to node 6 sequentially to calculate the $\mathrm{NRV}(m_i, r_2)$. Fig. 4.4 shows the $\mathrm{SI}(m_2, r_i)$

and NRV(m_2, r_i). In this case, a 0.01 kg mass is added on node 2 to identify the NRVs of nodes due to mass modification. Fig. 4.5 and 4.6 indicate results related to stiffness modifications in the same manner as the results related to mass modification shown in Fig. 4.3 and 4.4. Fig. 4.5 shows the SI$\left(k_{ij}, r_2\right)$ and NRV$\left(k_{ij}, r_2\right)$. Furthermore, a stiffness of 15,000 N/m is added on stiffnesses (k_{23}, k_{24}, k_{34}, k_{35}, k_{45}) to calculate the NRV$\left(k_{ij}, r_2\right)$. Fig. 4.6 shows the SI(k_{23}, r_i) and NRV(k_{23}, r_i) that represent sensitivity characteristics due to stiffness k_{23}. All the results indicate that the sensitivity indices exactly express the sensitivity characteristics of the system by showing that the NRVs (Fig. 4.3(b), 4.4(b), 4.5(b), 4.6(b)) agreed well with the SIs (Fig. 4.3(a), 4.4(a), 4.5(a), 4.6(a)) for all frequency ranges.

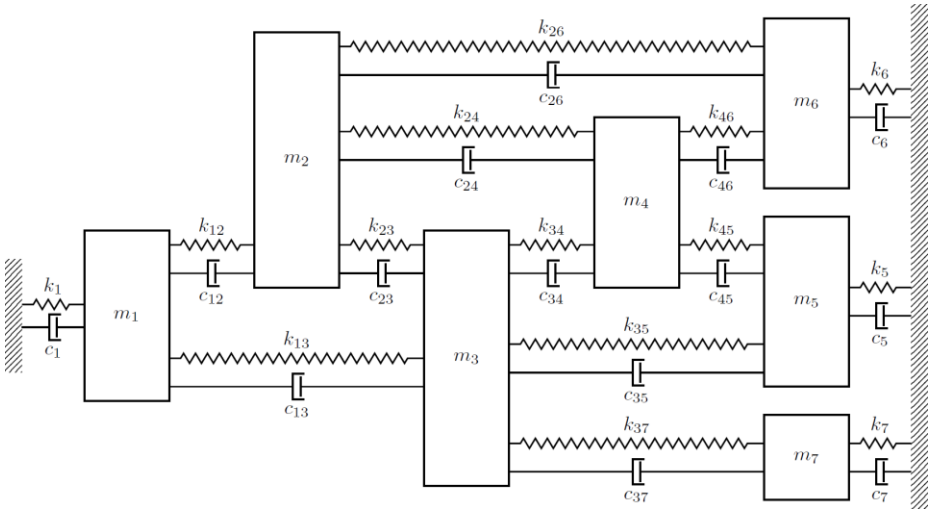

Figure 4.2 7-DOF discrete model

Table 4.1 System parameter properties of 7-DOF model

Mass (kg)	Stiffness ($\mathrm{N\,m^{-1}}$)		Damping ($\mathrm{N\,s\,m^{-1}}$)	
$m_1 = 30$	$k_1 = 10{\times}10^6$	$k_{35} = 4{\times}10^6$	$c_1 = 500$	$c_{35} = 200$
$m_2 = 9$	$k_{12} = 1{\times}10^6$	$k_{37} = 3{\times}10^6$	$c_{12} = 100$	$c_{37} = 300$
$m_3 = 15$	$k_{13} = 2{\times}10^6$	$k_{45} = 2.5{\times}10^6$	$c_{13} = 150$	$c_{45} = 125$
$m_4 = 12$	$k_{23} = 1.5{\times}10^6$	$k_{46} = 3.4{\times}10^6$	$c_{23} = 125$	$c_{46} = 400$
$m_5 = 27$	$k_{24} = 2{\times}10^6$	$k_5 = 8{\times}10^6$	$c_{24} = 300$	$c_5 = 400$
$m_6 = 15$	$k_{26} = 1.2{\times}10^6$	$k_6 = 6{\times}10^6$	$c_{26} = 300$	$c_6 = 210$
$m_7 = 24$	$k_{34} = 3.5{\times}10^6$	$k_7 = 7{\times}10^6$	$c_{34} = 275$	$c_7 = 320$

(a)

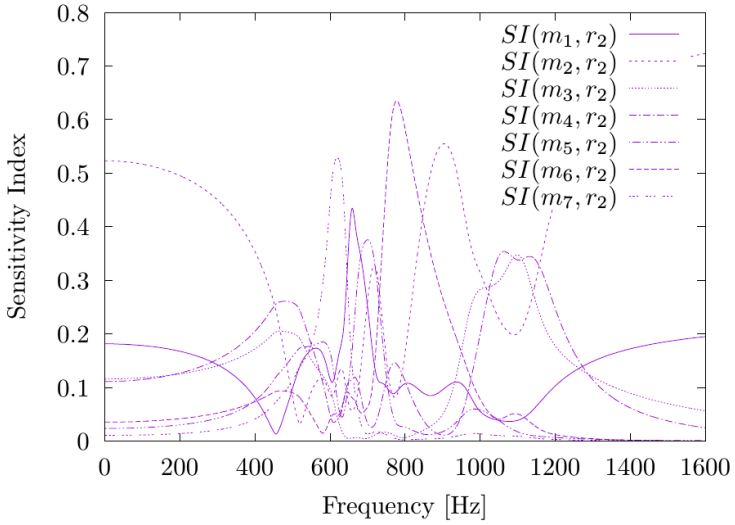

(b)

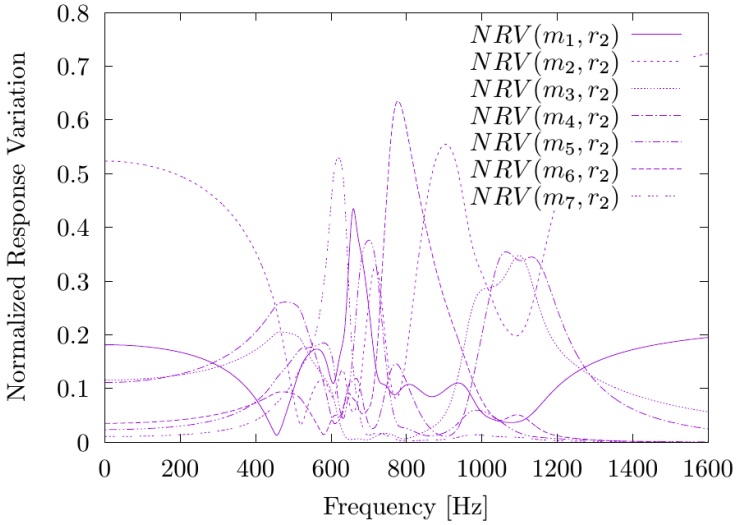

Figure 4.3 (a) Sensitivity index of node 2 with respect to mass on node ***i***, and (b) normalized response variations on node 2 due to small mass modification on node ***i***

(a)

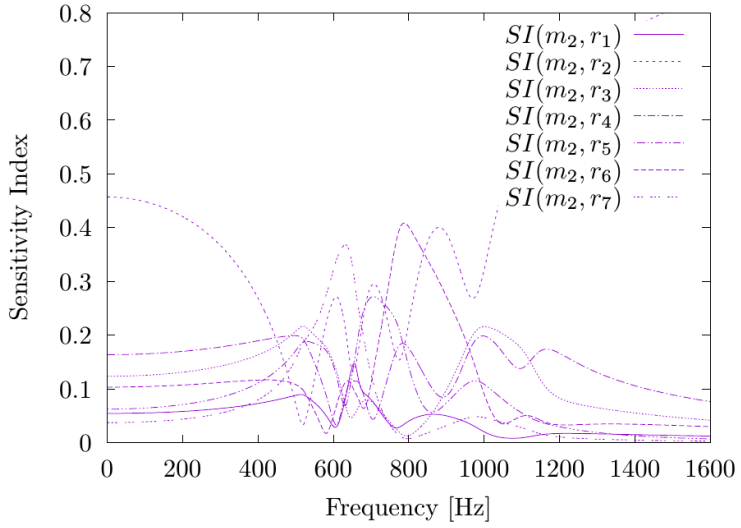

(b)

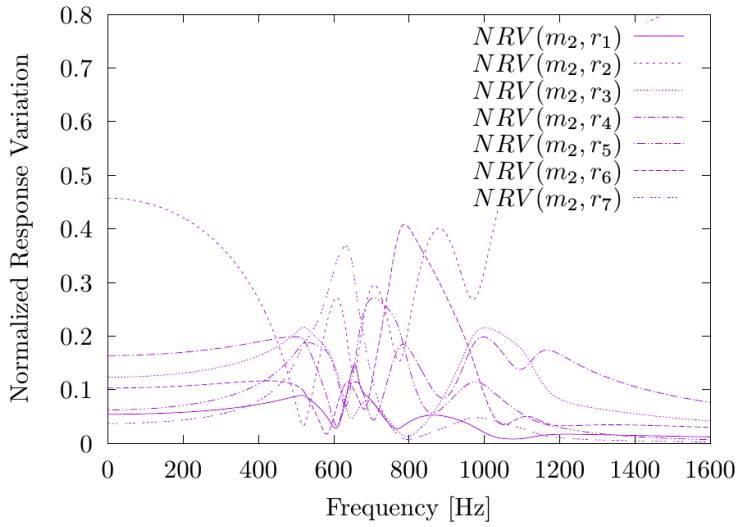

Figure 4.4 (a) Sensitivity index of node i with respect to mass on node 2, and (b) normalized response variations on node i due to small mass modification on node 2

(a)

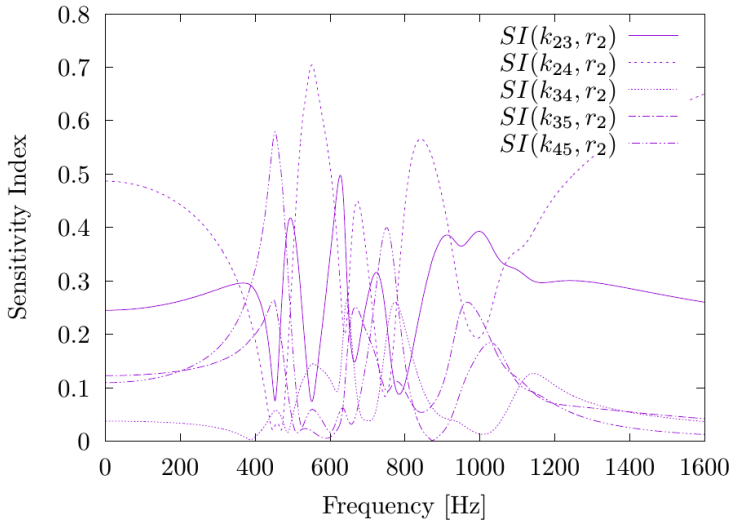

(b)

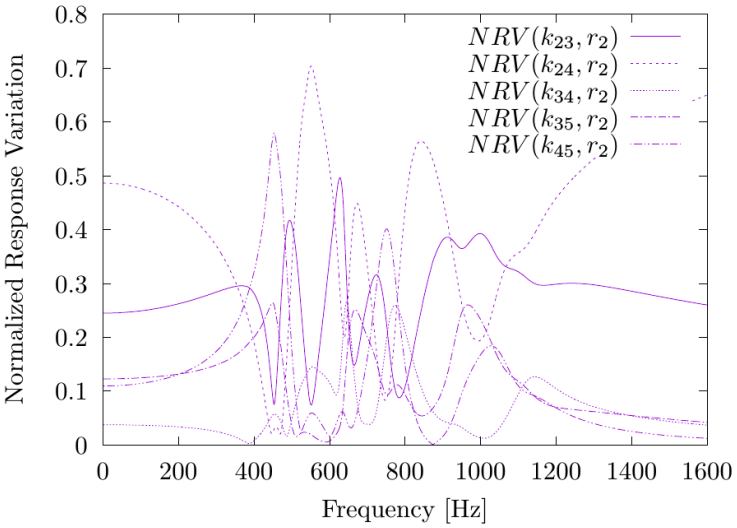

Figure 4.5 (a) Sensitivity index of node 2 with respect to stiffness between node i and node j, and (b) normalized response variations on node 2 due to small stiffness modification between node i and node j

(a)

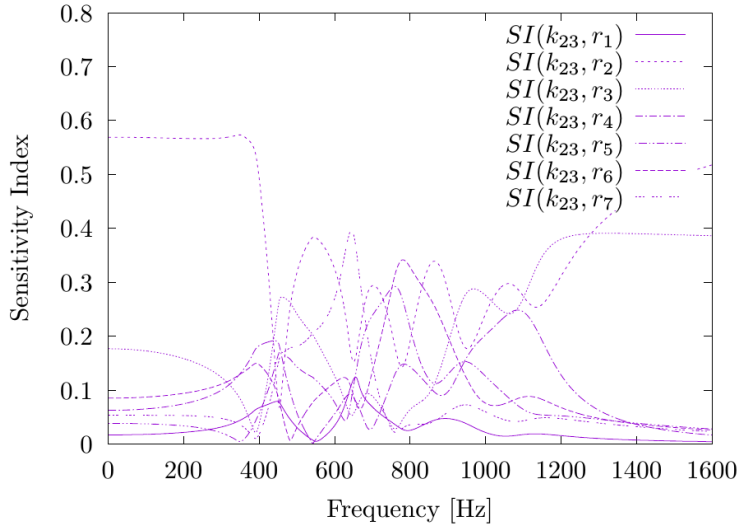

(b)

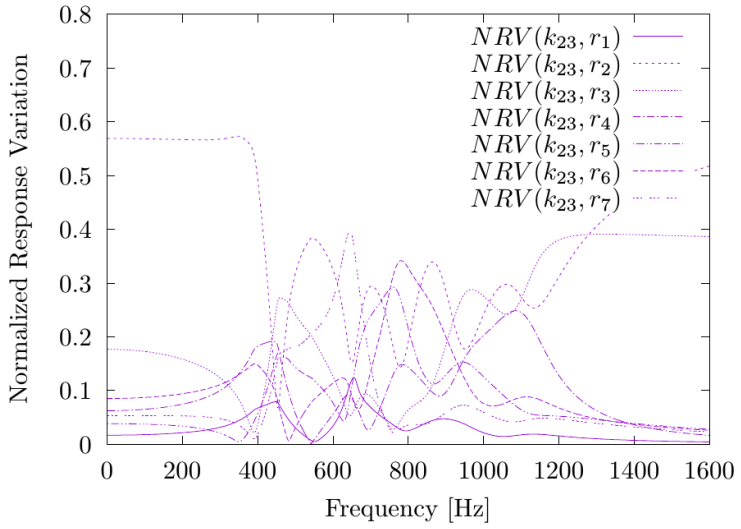

Figure 4.6 (a) Sensitivity index of node i with respect to stiffness between node 2 and node 3, and (b) normalized response variations on node i due to small stiffness modification between node 2 and node 3

4.3.2 Finite Beam Model

The proposed indices related to mass and stiffness are validated below numerically using two different models that are sufficiently simplified to be investigated. A single beam and two beams connected to each other with three stiffnesses are used to validate the indices with respect to mass and stiffness, respectively. It is assumed that the external force acts on node 1 and that only the z-directional accelerations in the beam models are used to validate the indices.

4.3.2.1 Results for Mass Variable

Only a single beam with boundary conditions satisfies the necessary conditions such that it can be used to validate the indices with respect to mass. Both sides of the beam model are simply supported by boundary conditions. Fig. 4.7(a) and 4.7(b) show the original numerical model and an example of a numerical model modified by adding a small concentrated mass to the node i, respectively to investigate the validity of the indices. A 0.0001 kg concentrated mass is added to achieve the normalized response variations used as indicators and a 20 N force acts on node 1 as an external force. The node numbers of the

beam model are denoted as 1 to 5 from left to right. Table 4.2 shows the properties of the numerical model shown in Fig. 4.7.

Fig. 4.8(a) and 4.8(b) show $\mathrm{SI}(m_i, r_2)$ and $\mathrm{NRV}(m_i, r_2)$. They correspond well for almost all frequency ranges. However, there are some frequency ranges at which the indicators do not match with the index, and these ranges approximately correspond to 189 Hz, 610 Hz, and 1300 Hz in Fig. 4.9(a) and 4.9(b). Specifically, $\mathrm{NRV}(m_2, r_i)$ denotes the normalized response variations with respect to the mass on node 2. It is necessary to obtain response variations due to the added mass when an external force acts on node 1. As shown in Fig. 4.10, H_{12} exhibits anti-resonance at the frequencies as explained above. This implies that the added mass on node 2 has little effect on the response variations at these frequencies. Thus, the variations obtained from the numerical beam model can have errors with respect to the anti-resonance frequencies of H_{12}. That is, the indices yield very reliable results with respect to sensitivity characteristics related to mass in all frequency ranges although there are discrepancies between the index and indicator at the anti-resonance frequency of H_{12}.

(a)

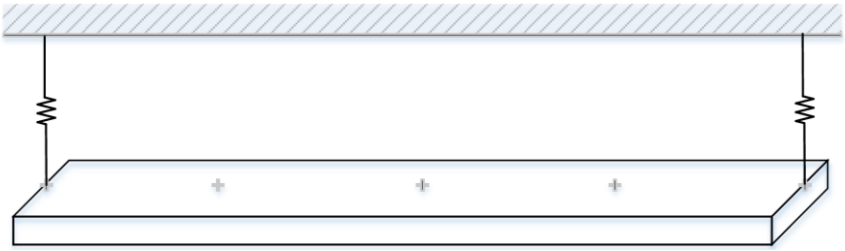

(b)

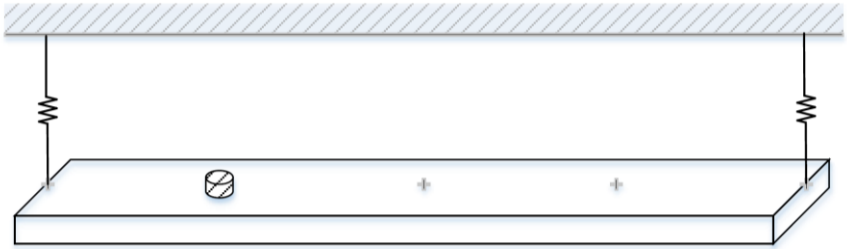

Figure 4.7 Beam structures: (a) Original, (b) after small mass modification

Table 4.2 Properties of beam model for validation of sensitivity indices with respect to mass

	Beam Model
Width (m)	0.05
Height (m)	0.015
Length (m)	0.5
Material	Steel
Young's modulus, E ($\mathrm{kg\,m^{-1}\,s^{-2}}$)	2.1×10^{11}
Poisson's ratio, nu	0.27
Mass density ($\mathrm{kg\,m^{-3}}$)	7850
Stiffness of left b.c ($\mathrm{N\,m^{-1}}$)	10^6
Stiffness of right b.c ($\mathrm{N\,m^{-1}}$)	5×10^6
Structural damping of left b.c ($\mathrm{N\,m^{-1}}$)	10^3
Structural damping of right b.c ($\mathrm{N\,m^{-1}}$)	5×10^3
Small concentrated mass added on node i (kg)	0.0001

(a)

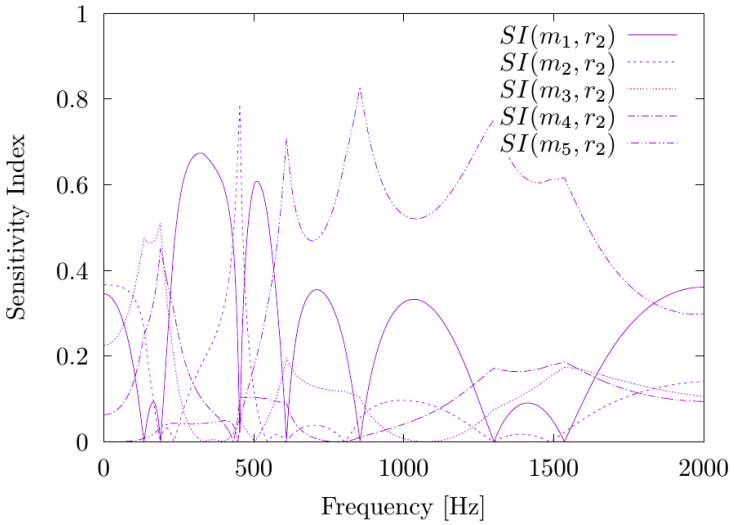

(b)

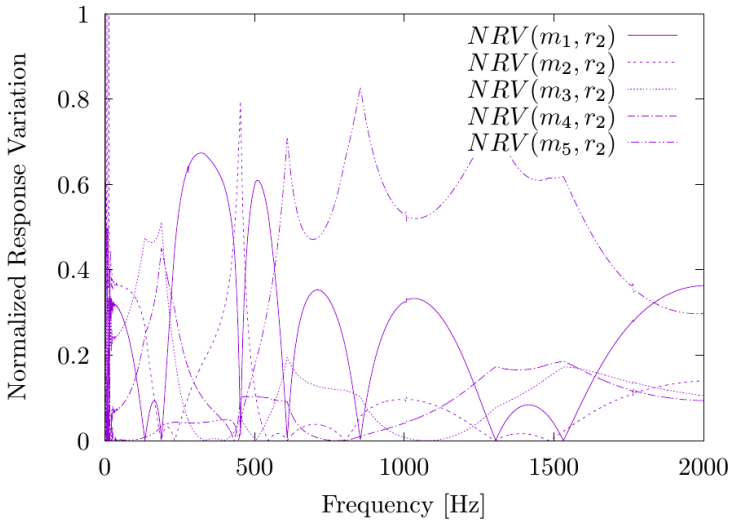

Figure 4.8 (a) Sensitivity index of node 2 with respect to mass on node i, and (b) normalized response variations on node 2 due to small mass modification on node i

(a)

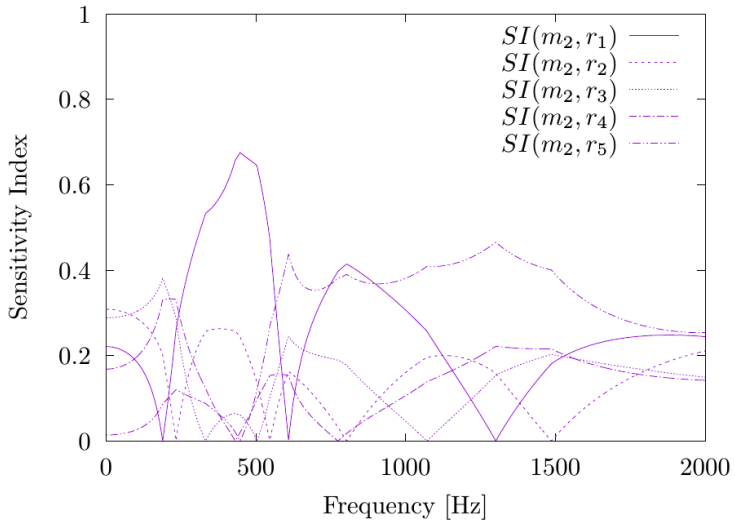

(b)

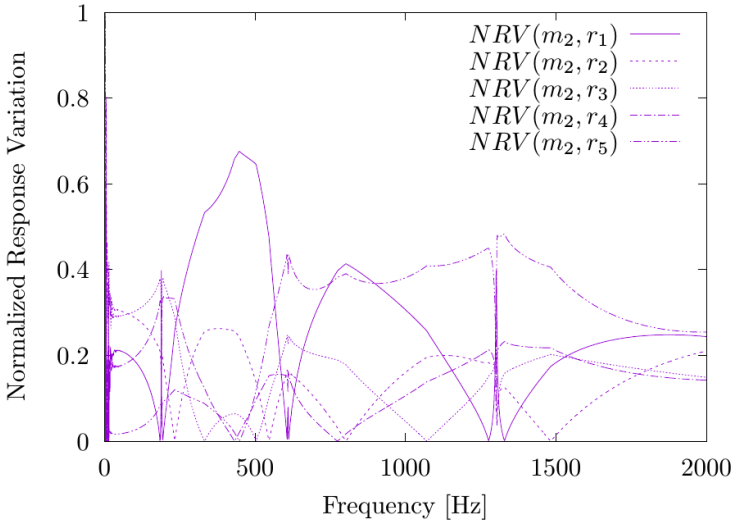

Figure 4.9 (a) Sensitivity index of node i with respect to mass on node 2, and (b) normalized response variations on node i due to small mass modification on node 2

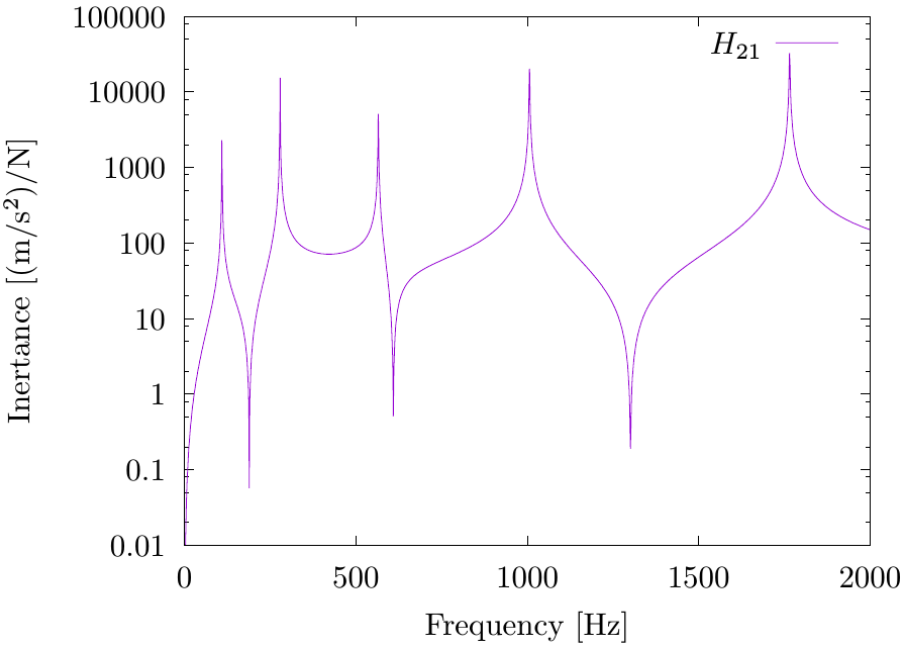

Figure 4.10 Frequency response function, H_{21}

4.3.2.2 Results for Stiffness Variable

Sensitivity with respect to stiffness is important in several practical conditions. The most common case involves that of the joint system. However, as it is difficult to precisely model a real joint system, a simplified model composed of joints represented by simple stiffness is used. The model involves two beams that are simply supported by grounding stiffnesses and are connected to each other using joint stiffness. Although this does not represent practical conditions, it does not have a problem in validating the indices related to stiffness. Fig. 4.11(a) and 4.11(b) show the original numerical model and an example of a numerical model modified by adding small stiffness to node i and node j, respectively to investigate the validity of the indices. A stiffness of 15,000 N/m is added to achieve normalized response variations used as indicators. The node numbers correspond to 1 to 5 from left to right in the upper beam and to 6 to 10 from left to right in the lower beam. Table 4.3 shows the properties of the numerical model shown in Fig. 4.11.

Fig. 4.12(a) and 4.12(b) show $\mathrm{SI}(k_{ij}, r_{10})$ and $\mathrm{NRV}(k_{ij}, r_{10})$, respectively. They correspond well in almost all frequency ranges. However, in the case of the $\mathrm{SI}(k_{27}, r_i)$ and $\mathrm{NRV}(k_{27}, r_i)$, there is also a discrepancy in the frequency range at approximately 1340 Hz. Unlike the mass modification case,

the response variations with respect to stiffness are affected by two nodes that are connected by the modified stiffness k_{27}. Thus the frequency ranges of discrepancy between the indices and indicators are related to H_{21} and H_{71}. The force caused by the modified stiffness (k_{27}) is the result of the difference between the accelerations a_2 and a_7. This indicates that the errors of NRV(k_{27}, r_i) can appear in the anti-resonance of differences between H_{21} and H_{71} in the numerical simulation. Fig. 4.15 shows the difference between H_{21} and H_{71}. Given that anti-resonance occurs at approximately 1340 Hz, the indicators exhibit errors in this frequency range. Thus, the index does not exhibit problems in any frequency range.

(a)

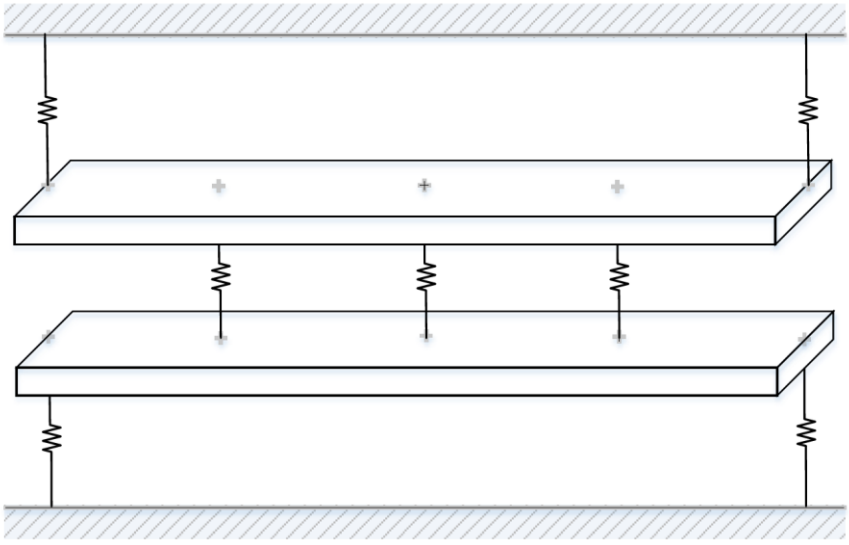

(b)

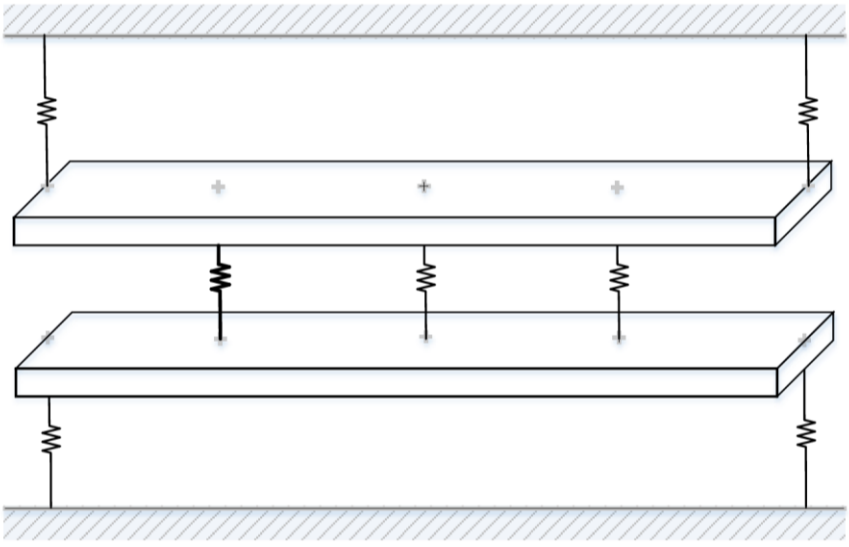

Figure 4.11 Beam structures: (a) Original, (b) after small stiffness modification

Table 4.3 Properties of beam model for validation of sensitivity indices with respect to stiffness

	Beam model
Stiffness of upper left b.c (N m^{-1})	10^6
Stiffness of upper right b.c (N m^{-1})	5×10^6
Stiffness of lower left b.c (N m^{-1})	6×10^6
Stiffness of lower right b.c (N m^{-1})	2×10^6
Structural damping of upper left b.c (N m^{-1})	10^3
Structural damping of upper right b.c (N m^{-1})	5×10^3
Structural damping of lower left b.c (N m^{-1})	6×10^3
Structural damping of lower right b.c (N m^{-1})	2×10^3
Stiffness between node 2 and node 7 (N m^{-1})	10^6
Stiffness between node 3 and node 8 (N m^{-1})	2×10^6
Stiffness between node 4 and node 9 (N m^{-1})	3×10^6
Small stiffness added on node i and node j (N m^{-1})	15,000

(a)

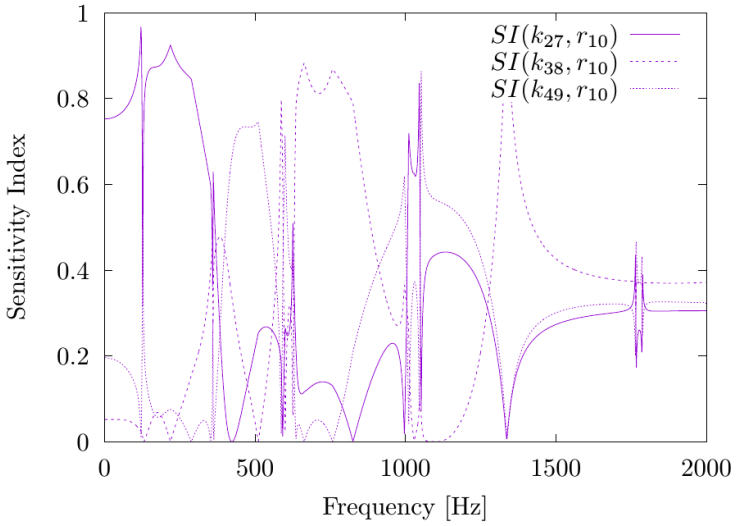

(b)

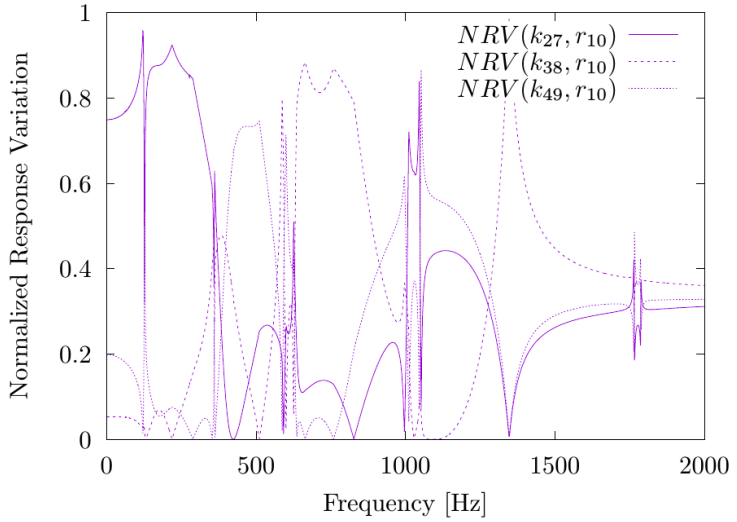

Figure 4.12 (a) Sensitivity index of node 10 with respect to stiffness between node i and node j, and (b) normalized response variations on node 10 due to small stiffness modification between node i and node j

(a)

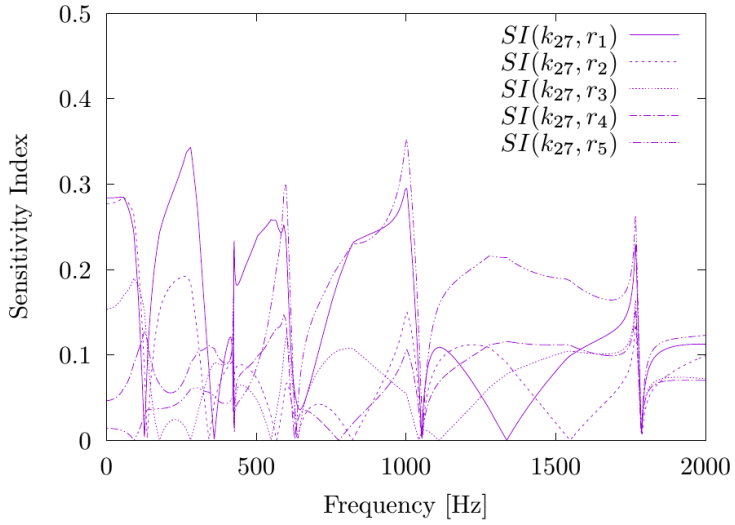

(b)

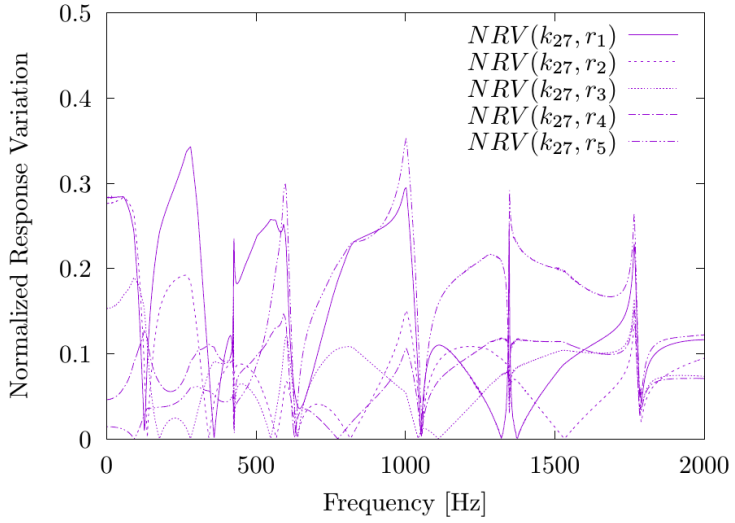

Figure 4.13 (a) Sensitivity index of node i (1~5) with respect to siffness between node 2 and node 7, and (b) normalized response variations on node i (1~5) due to small stiffness modification between node 2 and node 7

(a)

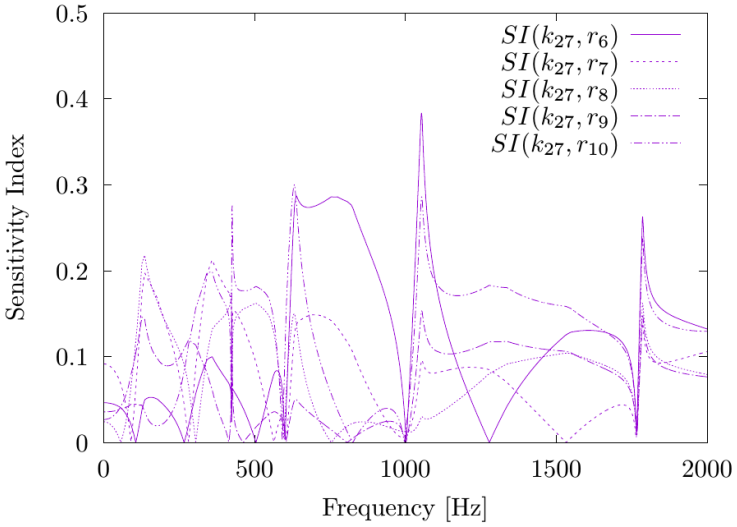

(b)

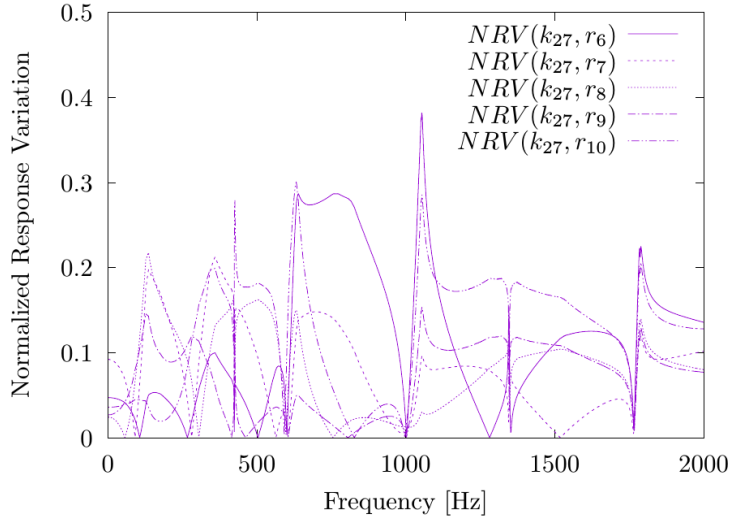

Figure 4.14 (a) Sensitivity index of node i (6~10) with respect to siffness between node 2 and node 7, and (b) normalized response variations on node i (6~10) due to small stiffness modification between node 2 and node 7

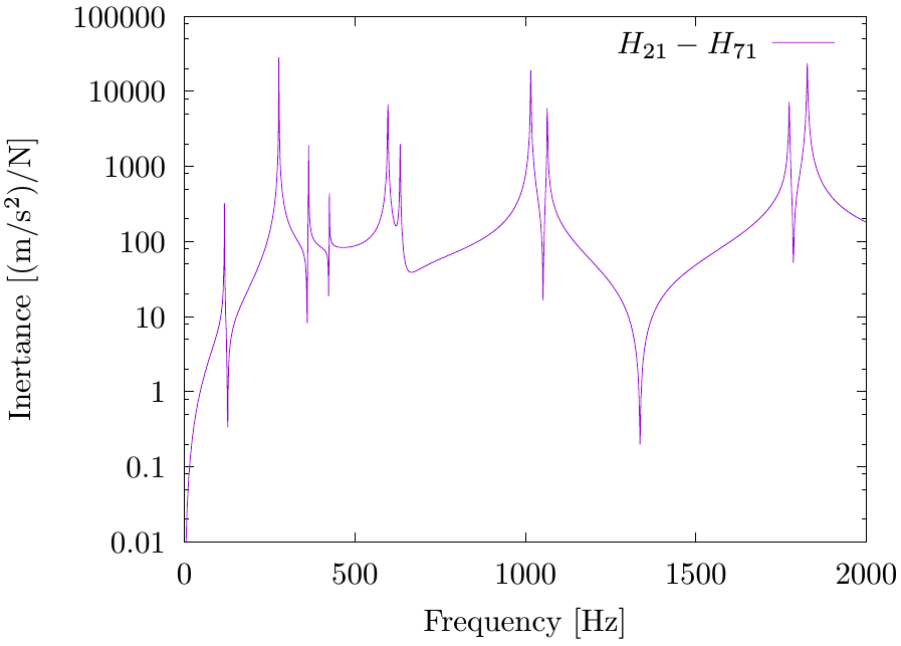

Figure 4.15 FRF difference between H_{21} and H_{71}

4.4 Summary and Conclusion

In this Chapter, new sensitivity indices are proposed to analyze the relative sensitivity of responses with respect to design variables using transmissibility. More reasonable information could be obtained by considering crosstalk effects between nodes. Two types of sensitivity indices are proposed with respect to design variables and defined as $\mathrm{SI}(V_i, R_k)$ and $\mathrm{SI}(V_k, R_i)$. Specifically, V and R are the variable and response, respectively. The indices provide information related to appropriate positions at which a small design modification can be applied and the manner in which the responses are mostly affected by the design variable at specific position. A 7-DOF discrete model is adopted to verify the indices. The indices are compared to indicators representing normalized response variations between the components before and after applying the small design modifications. Furthermore, two beam models are used to validate the indices with respect to mass and stiffness in more practical applications. The results in both cases indicate that the indices correspond well with the indicators at all frequencies. In conclusion, the proposed indices are validated and it is expected that the proposed indices will provide useful information of sensitivity characteristics to reduce vibrational problems in more practical conditions with easily measured response data.

CHAPTER 5

Conclusions

In this thesis, new approaches for boundary identification and relative sensitivity analysis by using transmissibility are presented. They are important parts in developing process of vibrational characteristic improvements. Because only responses are included in transmissibility, unlike FRFs that include input force measurements, the measurement errors caused by an incorrectly measured force can be excluded by adopting transmissibility to developing process.

The equation for estimating boundary properties is derived by investigating the difference in transmissibilities defined by the apparent masses under different conditions. Discrete models containing a single boundary condition and multiple boundary conditions are used for verification of the proposed method. Single boundary properties can be estimated by a very simple and intuitive process, while the multiple boundary properties can be estimated by using transmissibility matrix. The results from discrete models show that the properties are estimated well. In addition, a beam model is used to investigate whether the method can be expanded to be applicable to real structures. It has

been found that the boundary properties can be estimated with very good accuracy. Further, the effects of the numbers and positions of DOFs have been studied. The number of measuring DOFs and input DOFs should be expanded simultaneously for estimating the properties as accurately as possible, whereas only the number of measuring DOFs should be expanded, while the number of input DOFs are same as the number of boundary conditions, for estimating the properties efficiently. The robustness of the method also assessed by deriving the error equation with measurement noise. It was found that the method is robust to measurement noise by showing fairly reliable results over a wide frequency range.

The sensitivity indices of the response for positions of variables and the sensitivity indices of responses for positions of responses are developed to analyze relative sensitivity of responses. The indices are based on transmissibility. The former indicates the appropriate position where the design variable could be modified, while the latter indicates the effect of a specific design variable on the responses. Crosstalk effects are considered, and the indices are applicable for mass, stiffness, and damping. A 7-DOF discrete model and two numerical beam models are used to verify the indices by investigating whether the indices reflect the relative changes in response to small design modifications. It was found that the indices represent the relative

changes well by giving the reliable results in both cases.

As for future work, it would be desirable to consider rotational DOFs. The general derivation of the equations with the rotational DOFs is identical to that explained in the thesis. For including the rotational DOFs, some matrices should be expanded. Thus, the derived equations have no problem for including the rotational DOFs theoretically. However, the response data are used under practical conditions for utilizing the proposed method as shown in a validation applied to the continuous structure. This means that transmissibilities should be expressed using frequency response functions. Rotational DOFs can be included in H matrices. If translational DOFs and rotational DOFs are coupled weakly, the off-diagonal terms are removed. Then, the transmissibility matrix can be composed of only response data. It is possible to use the proposed method to estimate the boundary properties including rotational DOFs. In the general case, however, the transmissibility matrix has diagonal terms because of the coupling effect between translational DOFs and rotational DOFs. Although the coupling effect does not cause considerable deviation in joint identification according to reference [11], further study is needed. Thus, although the derived equation has no weak point in including the rotational DOFs theoretically, further research related to transmissibility characteristics between translational DOFs and rotational DOFs should be studied to utilize

the method more accurately using only response data under practical conditions because some studies about FRFs of rotational DOFs are not enough to be used in estimating boundary properties and relative sensitivity analysis with only response data.

REFERENCES

1. J.-S. Tsai, Y.-F. Chou, The identification of dynamic characteristics of a single bolt joint, *Journal of Sound and Vibration* **125** (3) (1988) 487-502.

2. J. Wang, C. Liou, Experimental identification of mechanical joint parameters, *Journal of Vibration and Acoustics* **113** (1) (1991) 28-36.

3. T. Yang, S.-H. Fan, C.-S. Lin, Joint stiffness identification using FRF measurements, *Computers & Structures* **81** (28) (2003) 2549-2556.

4. Y. Ren, C. Beards, Identification of joint properties of a structure using FRF data, *Journal of Sound and Vibration* **186** (4) (1995) 567-587.

5. D. Čelič, M. Boltežar, Identification of the dynamic properties of joints using frequency-response functions, *Journal of sound and Vibration* **317** (1) (2008) 158-174.

6. D. Čelič, M. Boltežar, The influence of the coordinate reduction on the identification of the joint dynamic properties, *Mechanical Systems and Signal Processing* **23** (4) (2009) 1260-1271.

7. M. Wang, D. Wang, G. Zheng, Joint dynamic properties identification with partially measured frequency response function, *Mechanical Systems and Signal Processing* **27** (2012) 499-512.

8. Ş Tol, et al., Dynamic characterization of bolted joints using FRF decoupling and optimization, *Mechanical Systems and Signal Processing* **54** (2015) 124-138.

9. H. Cao, S. Xi, W. Cheng, Model updating of spindle systems based on the identification of joint dynamics, *Shock and Vibrations* **2015** (2015) 10.

10. H. Hwang, Identification techniques of structure connection parameters using frequency response functions, *Journal of Sound and Vibration* **212** (3) (1998) 469-479.

11. M. Mehrpouya, E. Graham, S.S. Park, FRF based joint dynamics modeling and identification, *Mechanical Systems and Signal Processing* **39** (1) (2013) 265-279.

12. J. S. Arora, E. J. Haug, Methods of design sensitivity analysis in structural optimization, *AIAA Journal* **17** (9) (1979) 970-974.

13. V. Komkov, K. K. Choi, E. J. Haug, Design sensitivity analysis of structural systems, Academic press, 1986.

14. R. T. Haftka, H. Ma. Adelman, Recent developments in structural sensitivity analysis, *Structural Optimization* **1** (3) (1989) 137-151.

15. F. Van Keulen, R. Haftka, N. Kim, Review of options for structural design sensitivity analysis. part 1: Linear systems, *Computer Methods in Applied Mechanics and Engineering* **194** (30) (2005) 3213-3243.

16. K. K. Choi, N.-H. Kim, Structural sensitivity analysis and optimization 1: linear systems, Springer Science & Business Media, 2006.

17. R. Fox, M. Kapoor, Rates of change of eigenvalues and eigenvectors, *AIAA Journal* **6** (12) (1968) 2426-2429.

18. L. C. Rogers, Derivatives of eigenvalues and eigenvectors, *AIAA Journal* **8** (5) (1970) 943-944.

19. R. B. Nelson, Simplified calculation of eigenvector derivatives, *AIAA Journal* **14** (9) (1976) 1201-1205.

20. J. He, Sensitivity analysis and error matrix method using measured frequency response function(FRF) data, in: Proceedings of the 11th International Modal Analysis Conference (IMAC 11), Kissimmee, FL, 1993, pp. 1079-1082.

21. R. Lin, M. Lim, Derivation of structural design sensitivities from vibration test data, *Journal of Sound and Vibration* **201** (5) (1997) 613-631.

22. H. Jalali, B. T. Bonab, Nonlinearity identification using sensitivity of frequency response functions, *Journal of Vibration and Control* **19** (5) (2013) 787-800.

23. E. J. Haug, J. S. Arora, Design sensitivity analysis of elastic mechanical systems, *Computer Methods in Applied Mechanics and Engineering* **15** (1) (1978) 35-62.

24. Y. Zhang, A. Der Kiureghian, Dynamic response sensitivity of inelastic structures, *Computer Methods in Applied Mechanics and Engineering* **108** (1) (1993) 23-36.

25. Q. M, Liu, J. Zhang, L. B. Yan, Response sensitivity and hessian matrix analysis of planar frames subjected to earthquake excitation, *Finite Elements in Analysis and Design* **45** (10) (2009) 695-709.

26. Q. M. Liu, J. Zhang, L. B. Yan, A numerical method of calculating first and second derivatives of dynamic response based on gauss precise time step integration method, *European Journal of Mechanics A/Solids* **29** (3) (2010) 370-377.

27. Z. Lu, S. Law, Features of dynamic response sensitivity and its application in damage detection, *Journal of Sound and Vibration* **303** (1) (2007) 305-329.

28. J. W. Zhan, H. Xia, S. Y. Chen, G. De Roeck, Structural damage identification for railway bridges based on train-induced bridge responses and sensitivity analysis, *Journal of Sound and Vibration* **330** (4) (2011) 757-770.

29. P. G. Bakir, E. Reynders, G. De Roeck, Sensitivity-based finite element model updating using constrained optimization with a trust region algorithm, *Journal of Sound and Vibration* **305** (1) (2007) 211-225.

30. J. E. Mottershead, M. Link, M. I. Friswell, The sensitivity method in finite element model updating: a tutorial, *Mechanical Systems and Signal Processing* **25** (7) (2011) 2275-2296.

31. K. Koo, B. Pluymers, W. Desmet, S. Wang, Vibro-acoustic design sensitivity analysis using the wave-based method, *Journal of Sound and Vibration* **330** (17) (2011) 4340-4351.

32. U. Kirsch, P. Y. Papalambros, Accurate displacement derivatives for structural optimization using approximate reanalysis, *Computer Methods in Applied Mechanics and Engineering* **190** (31) (2001) 3945-3956.

33. U. Kirsch, M. Bogomolni, F. V. Keulen, Efficient finite difference design sensitivities, AIAA Journal **43** (2) (2005) 399-405.

34. M. Bogomolni, U. Kirsch, I. Sheinman, Efficient design sensitivities of structures subjected to dynamic loading, *International Journal of Solids and Structures* **43** (18) (2006) 5485-5500.

35. C. Su, R. Xu, Random vibration analysis of structures by a time-domain explicit formulation method, *Structural Engineering and Mechanics* **52** (2) (2014) 239-260.

36. Z. Hu, C. Su, T. Chen, H. Ma, An explicit time-domain approach for sensitivity analysis of non-stationary random vibration problems, *Journal of Sound and Vibration* **382** (2016) 122-139.

37. W. Liu, D. Ewins, Transmissibility properties of MDOF systems, in: Proceedings of the 16th International Modal Analysis Conference (IMAC 16), Santa Barbara, California, USA, 1998.

38. A. Ribeiro, J. Silva, N. Maia, On the generalisation of the transmissibility concept, *Mechanical Systems and Signal Processing* **14** (1) (2000) 29-35.

39. N. Maia, J. Silva, A. Ribeiro, The transmissibility concept in multi-degree-of-freedom systems, *Mechanical Systems and Signal Processing* **15** (1) (2001) 129-137.

40. K. Noumura, J. Yoshida, Method of transfer path analysis for vehicle interior sound with no excitation experiment, in: Proceedings of FISITA World Automotive Congress, Yokohama, Japan, 2006.

41. P. Gajdatsy, K. Janssens, L. Gielen, P. Mas, H. Van Der Auweraer, Critical assessment of operational path analysis: mathematical problems of transmissibility estimation, *Journal of the Acoustical Society of America* **123** (5) (2008) 3869.

42. P. Gajdatsy, K. Janssens, W. Desmet, H. Van Der Auweraer, Application of the transmissibility concept in transfer path analysis, *Mechanical Systems and Signal Processing* **24** (7) (2010) 1963-1976.

43. D. Tcherniak, A. Schuhmacher, Application of transmissibility matrix method to NVH source contribution analysis, in: Proceedings of the 27th International Modal Analysis Conference (IMAC 27), Orlando, Florida, USA, 2009.

44. D. De Klerk, A. Ossipov, Operational transfer path analysis: Theory, guidelines and tire noise application, *Mechanical Systems and Signal Processing* **24** (7) (2010) 1950-1962.

45. P. Guillaume, L. Hermans, H. van der Auweraer, Maximum likelihood identification of modal parameters from operational data, in: Proceedings of the 17th International Modal Analysis Conference (IMAC 17), Kissimmee, Florida, USA, 1999.

46. C. Devriendt, P. Guillaume, Identification of modal parameters from transmissibility measurements, *Journal of Sound and Vibration* **314** (1) (2008) 343-356.

47. W. Weijtjens, G. De Sitter, C. Devriendt, P. Guillaume, Operational modal parameter estimation of MIMO systems using transmissibility functions, *Automatica* **50** (2) (2014) 559-564.

48. I. G. Araújo, J. E. Laier, Operational modal analysis using SVD of power spectral density transmissibility matrices, *Mechanical Systems and Signal Processing* **46** (1) (2014) 129-145.

49. I. G. Araújo, J. E. Laier, Operational modal analysis approach based on multivariable transmissibility with different transferring outputs, *Journal of Sound and Vibration* **351** (2015) 90-105.

50. H.-P. Zhu, L. Mao, S. Weng, A sensitivity-based structural damage identification method with unknown input excitation using transmissibility concept, *Journal of Sound and Vibration* **333** (26) (2014) 7135-7150.

51. X. Li, Z. Peng, X. Dong, W. Zhang, G. Meng, A new transmissibility based indicator of local variation in structure

and its application for damage detection, *Shock and Vibration* **2015** (2015) 18.

52. Y.-L. Zhou, E. Figueiredo, N. Maia, R. Perera, Damage detection and quantification using transmissibility coherence analysis, *Shock and Vibration* **2015** (2015) 16.

53. Y. Lage, N. Maia, M. Neves, A. Ribeiro, Force identification using the concept of displacement transmissibility, *Journal of Sound and Vibration* **332** (7) (2013) 1674-1686.

54. V. Meruane, Model updating using antiresonant frequencies identified from transmissibility functions, *Journal of Sound and Vibration* **332** (4) (2013) 807-820.

55. E. Rustighi, S. Elliott, Force transmissibility of structures traversed by a moving system, *Journal of Sound and Vibration* **311** (1) (2008) 97-108.

56. A. P. Urgueira, R. A. Almeida, N. M. Maia, On the use of the transmissibility concept for the evaluation of frequency response functions, *Mechanical Systems and Signal Processing* **25** (3) (2011) 940-951.

57. R. Almeida, A. Urgueira, N. Maia, The use of transmissibility properties to estimate FRFs on modified structures, *Shock and Vibration* **17** (4, 5) (2010) 563-577.

58. C.-J. Kim, Y. J. Kang, B.-H. Lee, H.-J. Ahn, Design sensitivity analysis of a system under intact conditions using measured response data, *Journal of Sound and Vibration* **331** (13) (2012) 3213-3226.

59. D. J. Ewins, Modal testing: theory and practice, Research Studies Press Ltd, Baldock, Herfordshire, UK, 2000.

60. M. Imregun, D. Robb, D. Ewins, Structural modification and coupling dynamic analysis using measured FRF data, in: Proceedings of the 5th International Modal Analysis Conference (IMAC 5), London, England, 1987.

61. Y. Lage, M. Neves, N. Maia, D. Tcherniak, Force transmissibility versus displacement transmissibility, *Journal of Sound and Vibration* **333** (22) (2014) 5708-5722.

국 문 초 록

촘촘하게 결합되어 있는 시스템의 경우 가진기를 설치하거나 임팩트 힘을 정확하게 주기 힘들기 때문에, 잘못 측정된 힘에 의해 그 측정 오차가 발생한다. 힘 측정을 포함하는 주파수 응답 함수와 달리 전달율은 응답신호로만 정의되기 때문에 힘 측정으로 인한 오차 요인을 줄일 수 있다. 본 논문은 결합부 특성과 응답 민감도 특성과 같이 진동 특성 개발 과정에서 중요한 역할을 하는 연구들에 대한 새로운 접근법 연구이며, 결합부 특성을 파악하고 상대민감도 분석을 위한 지수를 제안하기 위해 주파수응답함수가 아닌 전달율 개념을 도입하였다. 결합부에 연결된 시스템과 그렇지 않은 시스템의 전달율 특성 차이를 통해 결합부 특성을 추정할 수 있다. 단일결합부와 다중결합부에 연결된 다자유도 시스템을 사용하여 제안된 방법을 검증하고, 연속시스템인 빔에 적용함으로써 실제 시스템에 대한 그 적용가능성을 확인하였다. 추정된 결합부 특성과 실제 결합부 특성비교를 통해 본 방법의 신뢰성을 확인하였으며, 더 나아가 실제 시스템 적용 시 발생할 수 있는 측정 오차에 대한 영향을 분석하여 강건성을 평가하였다. 이어서, 응답에 대한 상대 민감도 분석을 위해 전달율에 기초한 민감도 지수를 제안하였다. 시스템의 진동특성 개선에 대한 설계 변경 과정에서 상대 민감도 특성 분석은

매우 중요한 역할을 한다. 설계 변수에 대한 두가지 유형의 지수가 개발되었으며, 각 지수를 통해 설계변경이 필요한 위치를 선정할 수 있고 특정 위치의 설계변경이 각 응답들에 어떠한 영향을 주는지에 대한 분석이 가능하다. 개발된 지수가 설계변경에 대한 응답 변화를 잘 나타내 주는지 검증하기 위해 이산 시스템과 연속 시스템에 적용하였으며, 모든 주파수 범위에서 신뢰성 있는 결과를 확인하였다.

주요어 : 주파수 응답 함수, 전달율, 응답, 결합부 특성, 상대민감도, 민감도 지수, 설계변수

학 번 : 2011-20759